Check for updates

JGR Solid Earth

RESEARCH ARTICLE
10.1029/2022JB025228

Impact of Tropospheric Ties on UT1-UTC in GNSS and VLBI Integrated Solution of Intensive Sessions

Jungang Wang[1,2,3], Maorong Ge[1,2], Susanne Glaser[1], Kyriakos Balidakis[4], Robert Heinkelmann[1], and Harald Schuh[1,2]

[1]Space Geodetic Techniques, GeoForschungsZentrum (GFZ), Potsdam, Germany, [2]Technische Universität Berlin, Institut für Geodäsie und Geoinformationstechnik, Berlin, Germany, [3]Shanghai Astronomical Observatory, Chinese Academy of Sciences, Shanghai, China, [4]Earth System Modelling, GeoForschungsZentrum (GFZ), Potsdam, Germany

Key Points:

- Tropospheric ties are applied in a Global Navigation Satellite System–Very Long Baseline Interferometry (GNSS–VLBI) integrated solution analyzing VLBI intensive (INT) sessions from 2001 to 2021
- Length of Day (LOD) of IVS INT sessions shows a better agreement by 10%–30% when compared to GNSS LOD product, mainly due to gradient ties
- Gradient ties, especially the east one, introduce systematic biases of −3 to −5 μs in Universal Time 1-Coordinate Universal Time of IVS INT sessions

Supporting Information:

Supporting Information may be found in the online version of this article.

Correspondence to:

J. Wang,
wangjungang2009@yeah.net

Citation:

Wang, J., Ge, M., Glaser, S., Balidakis, K., Heinkelmann, R., & Schuh, H. (2022). Impact of tropospheric ties on UT1-UTC in GNSS and VLBI integrated solution of intensive sessions. *Journal of Geophysical Research: Solid Earth*, *127*, e2022JB025228. https://doi.org/10.1029/2022JB025228

Received 10 JUL 2022
Accepted 3 NOV 2022

Author Contributions:

Conceptualization: Jungang Wang
Formal analysis: Jungang Wang
Funding acquisition: Maorong Ge
Investigation: Jungang Wang, Maorong Ge, Susanne Glaser, Robert Heinkelmann
Methodology: Jungang Wang, Maorong Ge
Project Administration: Maorong Ge
Resources: Jungang Wang
Software: Jungang Wang, Maorong Ge
Supervision: Maorong Ge, Harald Schuh

© 2022. The Authors.
This is an open access article under the terms of the Creative Commons Attribution License, which permits use, distribution and reproduction in any medium, provided the original work is properly cited.

Abstract Very Long Baseline Interferometry (VLBI) intensive (INT) sessions are critical for the rapid determination and densification of Universal Time 1-Coordinate Universal Time (UT1-UTC), which plays an important role in satellite geodesy and space exploration missions and is not predictable over longer time scales. Due to the limited observation geometry of INT sessions with two to three stations observing about 1 hr, tropospheric gradients cannot be estimated, which degrades the UT1-UTC precision. We investigate the impact of tropospheric ties at Global Navigation Satellite Systems (GNSSs) and VLBI co-located stations in INT sessions from 2001 to 2021. VLBI and GNSS observations are combined on the observation level. The results are evaluated by using both UT1-UTC and Length of Day (LOD) from consecutive sessions. We demonstrate a better agreement of 10%–30% when comparing the derived LOD to GNSS LOD for INT1, INT2, and VGOS-2 sessions; whereas, the agreement is not improved when directly comparing UT1-UTC to the IERS Earth Orientation Parameters (EOPs) product, potentially because INT sessions also contribute to IERS EOP products. The major impact comes from tropospheric gradient ties, whereas applying zenith delay ties does not improve or even deteriorate UT1-UTC agreement. Gradient ties also introduce systematic biases in UT1-UTC by around −3 to −5 μs, except for the Russian INT sessions. Regression analysis shows that the east gradient introduces systematic effects in UT1-UTC for sessions involving Germany and USA (Hawaii), whereas for Germany–Japan and Russian sessions, the north gradient also contributes systematically.

Plain Language Summary Universal Time 1-Coordinate Universal Time (UT1-UTC) gives the time difference of UT1, defined by Earth's rotation, and UTC, defined by atomic clocks. UT1-UTC is essential for real-time navigation and space exploration. The variation of the first-order negative time derivative of UT1-UTC, Length of Day (LOD), is induced by mass redistribution, including tides of the solid Earth and oceans, the liquid core of the Earth and atmospheric variation, and climate events such as El Niño. Very Long Baseline Interferometry (VLBI) observing active galactic nuclei is the only space geodetic technique that can determine UT1-UTC unambiguously. The 1-hr intensive (INT) sessions, designed for the rapid determination and densification of UT1-UTC, are performed daily with two VLBI radio telescopes. Due to the limited observation geometry, tropospheric gradients cannot be modeled in INT sessions, deteriorating UT1-UTC estimates. We demonstrate an improvement of 10%–30% in LOD by applying tropospheric ties at VLBI and Global Navigation Satellite Systems co-locations, especially the tropospheric gradients ties. Tropospheric gradient ties also introduce a systematic effect of −3 to −5 μs on UT1-UTC, especially the east gradient. Our study shows that tropospheric ties should be adopted in future VLBI analysis for optimal UT1-UTC products.

1. Introduction

Earth Orientation Parameters (EOPs) describe the change of the orientation of the Earth with respect to space and give the transformation between the International Celestial Reference Frame (Charlot et al., 2020) and the International Terrestrial Reference Frame (Altamimi et al., 2016). Accurate EOP information is important for positioning and navigation on the Earth and for space exploration missions, in particular for real-time applications. Currently, the EOPs are determined mainly by four space geodetic techniques including Global Navigation Satellite Systems (GNSSs) and Very Long Baseline Interferometry (VLBI) (Bizouard et al., 2018). The latter realizes uniquely the celestial pole offsets and Universal Time 1-Coordinate Universal Time (UT1-UTC), thanks to its precise observation to Active Galactic Nuclei (AGN). The 24-hr VLBI sessions are usually conducted two or three times per week with networks of globally distributed radio telescopes, and provide high-precision

21699356, 2022, 11, Downloaded from https://agupubs.onlinelibrary.wiley.com/doi/10.1029/2022JB025228 by Helmholtz-Zentrum Potsdam GFZ, Wiley Online Library on [28/11/2022]. See the Terms and Conditions (https://onlinelibrary.wiley.com/terms-and-conditions) on Wiley Online Library for rules of use; OA articles are governed by the applicable Creative Commons License

21699356, 2022, 11, Downloaded from https://agupubs.onlinelibrary.wiley.com/doi/10.1029/2022JB025228 by Helmholtz-Zentrum Potsdam GFZ, Wiley Online Library on [28/11/2022]. See the Terms and Conditions (https://onlinelibrary.wiley.com/terms-and-conditions) on Wiley Online Library for rules of use; OA articles are governed by the applicable Creative Commons License

Validation: Jungang Wang
Visualization: Jungang Wang
Writing – original draft: Jungang Wang, Maorong Ge, Susanne Glaser, Kyriakos Balidakis, Robert Heinkelmann, Harald Schuh
Writing – review & editing: Jungang Wang, Maorong Ge, Susanne Glaser, Kyriakos Balidakis, Robert Heinkelmann, Harald Schuh

EOP estimates, for instance, with a precision of about 5 μs for UT1-UTC (Böckmann et al., 2010; Gambis & Luzum, 2011). However, 24-hr sessions usually have a latency of about 2 weeks due to the data transportation and processing. The latency prohibits the optimal support of the short-term EOP prediction, especially in the case of UT1-UTC, which exhibits rapid variations caused by various geophysical excitations. Hence, the UT1-UTC precision for 10-day prediction is only around 1 ms (Johnson et al., 2005; Kalarus et al., 2010; Niedzielski & Kosek, 2007; Ray, 1996), which is equivalent to an 0.5 m arc on the Earth's surface.

For the rapid determination of UT1-UTC, intensive (INT) sessions using two to three VLBI radio telescopes observing for 1 hr have been conducted since 1984 (Robertson et al., 1985). These INT sessions are designed to be particularly sensitive to UT1-UTC due to the long east-west extension of the involved baseline, and the short observing time enables quick data transportation and processing. They also contribute to the densification of daily UT1-UTC of the IERS EOP products, which are commonly used to investigate geophysical pheonomeon (Duan & Huang, 2020).

Since 2001, two types of INT sessions have been coordinated by the International VLBI Service (IVS) (Nothnagel et al., 2016), and the results are available within hours after observing (Sekido et al., 2008). INT1 sessions are observed at around 18:30 UT from Monday to Friday employing radio telescopes in Kokee Park (Hawaii, USA) and Wettzell (Germany), and INT2 sessions are observed at 07:00 UT on Saturdays and Sundays between radio telescopes in Tsukuba (Japan) and Wettzell. INT3 sessions between radio telescopes in Tsukuba, Ny-Ålesund (Norway), and Wettzell are observed on Mondays at around 07:00 UT, bridging the gap between Sunday morning and Monday afternoon (Luzum & Nothnagel, 2010). In addition, VLBI intensive sessions are performed in USA and Russia to provide UT1-UTC in support of their national GNSS. The Russian INT sessions (RuI) (Shuygina et al., 2019) are observed daily since 2012, between Badary (Eastern Siberia), Svetloe (St. Petersburg), and Zelenchukskaya (Northern Caucasus). The observations are usually available within hours after observing (ftp://quasar.ipa.nw.ru/). Recently, VLBI stations equipped with the new VLBI Global Observing System (VGOS) technology were developed, which utilize very fast-slewing telescopes and broadband receiving systems (Niell et al., 2018; Petrachenko et al., 2012), and thus, provide more observations per time with higher precision. These VGOS stations participate in INT observing, such as VGOS-B sessions with baselines between Ishioka and the Onsala twin telescopes (Haas et al., 2021), and VGOS-2 sessions between the KOKEE12M telescope in Kokee Park and WETTZ13S telescope in Wettzell. Both IVS and RuI contribute to the International Earth Rotation Service (IERS) combined EOP product, for example, IERS EOP C04 (Bizouard et al., 2018).

Due to the design of two to three VLBI radio telescopes forming long east-west baselines and observing for 1 hr, INT sessions have limited observation geometry, as the observations are concentrated on a small slice of the sky that is in common view of the stations. To achieve robust estimates, a special processing strategy is followed. Coordinates of ground stations and AGN are fixed to the a priori values, and only UT1-UTC is estimated while polar motion and celestial pole offsets are fixed. Persistent efforts were made to investigate and improve UT1-UTC estimates based on INT sessions, including optimized scheduling strategies (Artz et al., 2012; Baver & Gipson, 2020; Gipson & Baver, 2015; Kareinen et al., 2017; Schartner et al., 2021, 2022), the impact of a priori EOP (mainly polar motion and celestial pole offsets) (Malkin, 2011; Nothnagel & Schnell, 2008) and seasonal station motions (Malkin, 2013), automated processing (Hobiger et al., 2011; Kareinen et al., 2015), and the combination with GNSS (Hellmers et al., 2019; Thaller et al., 2008).

Another important factor for INT session analyses is the atmospheric refraction modeling, especially tropospheric gradients which cannot be estimated due to the limited geometry, consequently causing systematic errors in UT1-UTC (Nilsson et al., 2011). On the one hand, zenith tropospheric delays (ZTDs) from Numerical Weather Models (NWM) agree with those from VLBI at the level of 1–2 cm (Heinkelmann et al., 2007; Soja et al., 2015; Teke et al., 2011, 2012) and can be used to improve the analysis of INT sessions (Böhm et al., 2010; Landskron & Böhm, 2019; Nafisi et al., 2012), where slight improvements are achieved. On the other hand, ZTD of GNSS agree with those of VLBI at the level of 4–6 mm (Puente et al., 2021; Teke et al., 2013; Wang, 2021) and can also be used in VLBI analysis. Teke et al. (2015) investigated the impact of using tropospheric gradients from GNSS in INT1 and INT2 sessions with data from 2008 to 2014 and demonstrated an improvement of up to 1 μs when compared to GNSS Length of Day (LOD, the negative time derivative of UT1-UTC). Nilsson et al. (2017) demonstrated that using GNSS tropospheric gradients with proper weights, UT1-UTC of INT sessions from 2002 to 2015 is improved by 5% when compared to concurrent 24-hr sessions, and the corresponding LOD is improved by 12% when compared to GNSS LOD. Applying tropospheric ties between GNSS and VLBI can also improve

21699356, 2022, 11, Downloaded from https://agupubs.onlinelibrary.wiley.com/doi/10.1029/2022JB025228 by Helmholtz-Zentrum Potsdam GFZ, Wiley Online Library on [28/11/2022]. See the Terms and Conditions (https://onlinelibrary.wiley.com/terms-and-conditions) on Wiley Online Library for rules of use; OA articles are governed by the applicable Creative Commons License

Table 1
List of Very Long Baseline Interferometry (VLBI) Radio Telescopes in Intensive (INT) Sessions and the Global Navigation Satellite System (GNSS) Co-Location Stations Investigated in This Study

VLBI radio telescope			
IVS name	IVS code	GNSS	Location
BADARY	Bd	BADG	Badary, Eastern Siberia, Russia
ISHIOKA	Is	ISHI	Ishioka, Japan
KOKEE	Kk	KOKB	Kokee Park, Hawaii, USA
KOKEE12M	K2	KOKB	Kokee Park, Hawaii, USA
KASHIM34	Kb	KSMV	Kashima, Japan
MK-VLBA	Mk	MKEA	Mauna Kea, Hawaii, USA
SVETLOE	Sv	SVTL	Svetloe, Leningrad, Russia
TSUKUB32	Ts	TSKB	Tsukuba, Japan
WETTZ13N	Wn	WTZR	Wettzell, Germany
WETTZ13S	Ws	WTZR	Wettzell, Germany
WETTZELL	Wz	WTZR	Wettzell, Germany
ZELENCHK	Zc	ZECK	Zelenchukskaya, Northern Caucasus, Russia

Note. The horizontal and vertical distances between GNSS and VLBI co-located stations are all within 300 and 20 m, respectively.

the VLBI station coordinates and EOPs of 24-hr sessions (Diamantidis et al., 2021; Hobiger & Otsubo, 2014; Krügel et al., 2007; Wang, 2021; Wang et al., 2022).

In this study, we investigate the impact of GNSS–VLBI tropospheric ties on UT1-UTC estimates of INT sessions. Unlike previous studies where GNSS and VLBI observations were processed separately using different software, such as Teke et al. (2015) and Nilsson et al. (2017), we process GNSS and VLBI observations simultaneously with a common least-squares estimator. Such a rigorous combination on the observation level allows for the highest consistency between GNSS and VLBI in terms of modeling, parameterization, and estimation. Our previous study (Wang et al., 2022) shows that the VLBI 24-hr sessions benefit from the tropospheric ties in such an integrated solution, as both the VLBI TRF and all EOP components are improved. We thus extend the method to INT sessions over 20 years. Unlike the 24-hr sessions with a global network, which mainly serve for reference frames and EOP determination, the INT sessions are only for UT1-UTC estimation and has its own limitation and corresponding special processing strategy, especially in tropospheric delay modeling. We thus aim at investigating (a) whether the tropospheric ties can improve UT1-UTC and (b) which tropospheric component could cause systematic effects and how large it is. The latter one also shows the systematic biases in the current IVS INT products.

Moreover, our investigation includes not only INT1 and INT2 between Tsukuba and Wettzell, but also INT2 between Ishioka and Wettzell and between Mauna Kea and Wettzell, VGOS-2, and RuI, which have not been thoroughly studied. We evaluate our results using not only the IERS EOP products but also GNSS LOD, including that of the International GNSS Service (IGS) (Johnston et al., 2017) combination and the Center for Orbit Determination in Europe (CODE, hereafter COD). Last but not the least, we quantify the impact of tropospheric zenith delay and gradients on UT1-UTC in various types of INT sessions using multiple linear regression analysis.

Following this introduction, the various INT sessions are presented in Section 2, together with data processing strategies of VLBI and GNSS observations. In Section 3 we evaluate the agreement of UT1-UTC and LOD with both IERS EOP 14C04 (Bizouard et al., 2018) and GNSS LOD. Section 4 concludes this manuscript by summarizing major findings and presenting future perspectives.

2. Data and Method

2.1. VLBI Intensive Sessions

This section describes the types of INT sessions grouped by network geometry. The station information is given in Table 1 and Figure 1. The number of sessions is given in Section 3. Note that INT1 usually refers to sessions observed from Monday to Friday at around 18:30 or 18:45 UTC, INT2 sessions refer to sessions observed on Saturday and Sunday at around 07:30 UTC.

The first group is between radio telescopes in Kokee Park and Wettzell, including KkWz (2-char station code of IVS) INT1 between KOKEE and WETTZELL (8-char station name of IVS, see also Table 1) from 2001 to 2021, K2Ws VGOS-2 between KOKEE12M and WETTZ13S in 2020 and 2021, and a few KkWnWz INT1 sessions between KOKEE, WETTZELL and WETTZ13N from 2017 to 2019.

The second group is between radio telescopes in Japan and Germany, mostly observed on weekends as INT2, including TsWz INT2 between TSUKUB32 and WETTZELL from 2004 to 2016 and IsWz between ISHIOKA and WETTZELL from 2016 to 2021, and a few KbWz sessions between KASHIM34 and WETTZELL from 2007 to 2018.

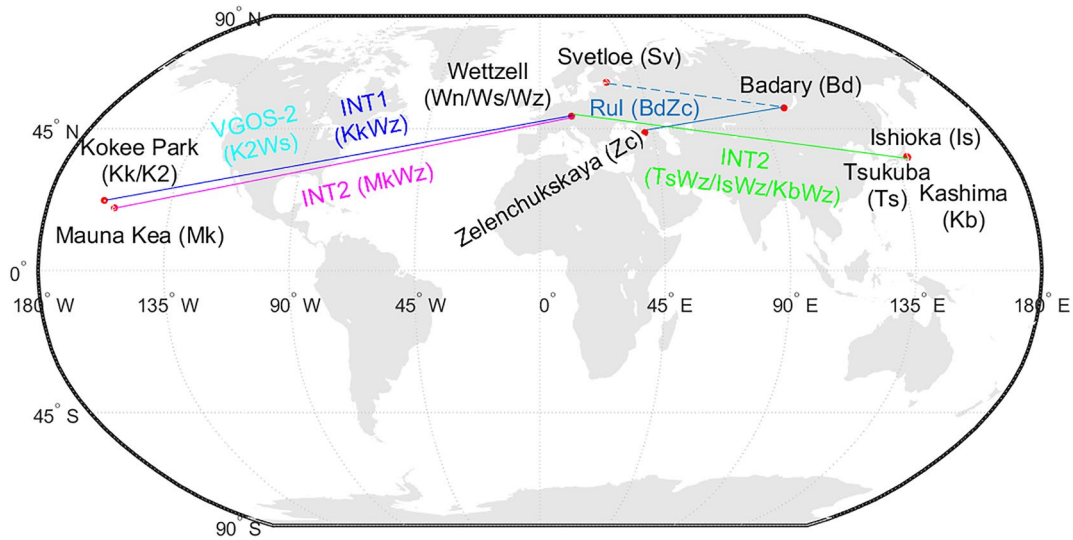

Figure 1. Intensive sessions investigated in this study and the corresponding geographical distribution of Very Long Baseline Interferometry radio telescopes.

In addition, the MkWz sessions between MK-VLBA and WETTZELL are observed mostly at 07:30 UTC on weekends as INT2, or occasionally at 18:30 UTC on weekdays as INT1, from 2019 to 2021. They are referred to as INT2 in this study.

The last group refers to the RuI, including BdZc between BADARY and ZELENCHK from 2010 to 2021, and BdSv between BADARY and SVETLOE. Most of the RuI are observed at around 19:00 UTC.

Note that we classify the sessions based on the baseline geometry instead of the observing time. Occasionally, the TsWz, IsWz, and MkWz baselines are observed on weekdays and labeled as INT1, and very rarely the KkWz baseline is observed on weekends. In this study, all the sessions of KkWz are referred to as INT1, and those of TsWz, IsWz, and MkWz as INT2.

2.2. Data Processing Strategy

The GNSS and VLBI observations are processed using the Positioning And Navigation Data Analyst (PANDA) software (Liu & Ge, 2003). PANDA is a GNSS data processing tool, capable of precise GNSS data analysis including orbit determination of multi-GNSS satellites (He et al., 2013; Liu et al., 2016) and LEO (Geng et al., 2008), real-time precise clock estimation (Zuo et al., 2021), and precise positioning and atmospheric sounding (Penna et al., 2018; Wang & Liu, 2019; Wang et al., 2019). It was recently upgraded to process VLBI and SLR observations (Wang, 2021; Wang et al., 2022), aiming at the goal of multi-technique integrated processing on the observation level.

Table 2 gives the data processing strategy. Note that GNSS and VLBI observations are always processed by a common least-squares estimator. We adopt a module of the Potsdam Open Source Radio Interferometry Tool (Schuh et al., 2021) to read VGOS-DB files and output the observations into NGS-card format for sessions after 2017 as the VGOS-DB format is adopted by IVS for this period.

2.3. Modeling Atmospheric Refraction

In GNSS and VLBI data analysis, the tropospheric delay $L(e,\alpha)$ in the slant direction with elevation e and azimuth α can be described as

$$L(e,\alpha) = mf_h(e)\cdot \mathrm{ZHD} + mf_w(e)\cdot(\mathrm{ZWD}_0 + \Delta\mathrm{ZWD}) + mf_g(e)\cdot(\cos(\alpha)\cdot \mathrm{GN} + \sin(\alpha)\cdot GE) \quad (1)$$

where ZHD and ZWD_0 denote the a priori zenith hydrostatic and wet delays (ZHD and ZWD), respectively; ΔZWD is the residual ZWD that is estimated; $mf_h(e)$ and $mf_w(e)$ are the corresponding hydrostatic and wet

21699356, 2022, 11, Downloaded from https://agupubs.onlinelibrary.wiley.com/doi/10.1029/2022JB025228 by Helmholtz-Zentrum Potsdam GFZ, Wiley Online Library on [28/11/2022]. See the Terms and Conditions (https://onlinelibrary.wiley.com/terms-and-conditions) on Wiley Online Library for rules of use; OA articles are governed by the applicable Creative Commons License

21699356, 2022, 11, Downloaded from https://agupubs.onlinelibrary.wiley.com/doi/10.1029/2022JB025228 by Helmholtz-Zentrum Potsdam GFZ, Wiley Online Library on [28/11/2022]. See the Terms and Conditions (https://onlinelibrary.wiley.com/terms-and-conditions) on Wiley Online Library for rules of use; OA articles are governed by the applicable Creative Commons License

Table 2
Processing Strategy of Global Navigation Satellite System (GNSS) and Very Long Baseline Interferometry (VLBI) Integrated Solution of Intensive (INT) Sessions

Item	VLBI	GNSS
Mode	Single-session solution	Daily Precise Point Positioning (PPP) mode
Observable	All S-band ionosphere-free calibrated X-band group delays with the quality code "0"	Un-differenced ionosphere-free linear combination of GPS L1 and L2 phase and pseudo-range observations
Weighting	Constant (0.01 m) + observation noise + ionospheric delay noise	0.01 and 1.0 m for ionosphere-free combined phase and range, respectively; elevation-dependent down-weighting for elevation $e < 30°$: $1/(2 \sin e)$
Cut-off elevation	No	5°
Celestial parameters	AGN coordinates fixed to ICRF3 (Charlot et al., 2020)	Satellite orbits and clocks fixed to the IGS 2nd reprocessing (before 2014) and operational products (after 2014)
Terrestrial parameters	Fixed to ITRF2014 (Altamimi et al., 2016) or Mikschi et al. (2021)	Estimated as daily constant
Clock	Linear function	Epoch-wise white noise
Ionospheric delay	First-order correction from observation file, no higher-order considered	First-order corrected by ionosphere-free combination, no higher-order considered
Instrument-related	Thermal deformation and axis offset corrected, cable calibration from observation file	Receiver and satellite PCV&PCO corrected using IGS14.atx (Rebischung & Schmid, 2016), differential code bias from COD product
EOP estimation	Polar motion and celestial pole offsets fixed to IERS EOP 14C04, UT1-UTC estimated as constant	No
Ephemeris	JPL DE405	
Station displacements	IERS 2010 Conventions (Petit & Luzum, 2010) adopted for solid Earth tides, ocean tides, pole tide, ocean pole tide, and S1-S2 tidal atmospheric pressure loading	
EOP modeling	A priori value from the IERS EOP 14C04; sub-daily models follow the IERS 2010 Conventions	

mapping functions. GN and GE are the north and east total gradients, respectively, and $mf_g(e)$ is the gradient mapping function.

In this study, the 6-hourly sampled VMF3 station-specific product is used to provide a priori ZHD and ZWD, and VMF3 is used for mapping functions (Landskron & Böhm, 2017). Residual ZWD and gradients are estimated as 1-hourly piece-wise-constant, and the Chen and Herring (1997) gradient mapping function is adopted.

For co-located GNSS and VLBI stations, the tropospheric delay can be considered as the same after considering the topography-related and instrument-related differences. We correct the first by using VMF3 station-specific product (Landskron & Böhm, 2017) for a priori zenith delays and mapping functions, whereas the latter is ignored in INT sessions, following previous studies (Nilsson et al., 2017; Teke et al., 2015). Unlike the 24-hr session analysis where instrument-related tropospheric tie biases can be estimated as unknown (Diamantidis et al., 2021; Hobiger & Otsubo, 2014; Wang et al., 2022), it is not optimal to do so in INT sessions. The reason is that INT sessions with one-hour observations from two to three stations have limited observation geometry, and estimating one bias for each tropospheric component per session has the same effect as not applying any tropospheric ties. As the height-related tropospheric ties are applied by using the a priori delays from VMF3, we tightly constrain the residual ZWD and gradients at co-located GNSS and VLBI stations to be equal using pseudo-observations, with an uncertainty of 0.01 mm.

We investigate different scenarios including (a) VLBI stations without and with tropospheric gradient modeling and estimation, coded as "G0" and "G1", respectively, and (b) different options of applying tropospheric ties between GNSS and VLBI, "NT" for not applying any ties, "ZT" for ZTD ties only, "GT" for gradient ties only, and "AT" for atmospheric ties applied, that is, both ZTD and gradient ties. Note that when tropospheric gradients are estimated for VLBI stations, gradient ties are always applied since gradients cannot be very well estimated using VLBI-only observations in INT sessions. Concluding, the following four scenarios are designed.

- G0NT: no tropospheric gradients for VLBI stations, no ties applied.
- G0ZT: no tropospheric gradients for VLBI stations, ZTD ties applied.
- G1GT: tropospheric gradient ties applied between GNSS and VLBI.
- G1AT: both ZTD and gradient ties applied between GNSS and VLBI.

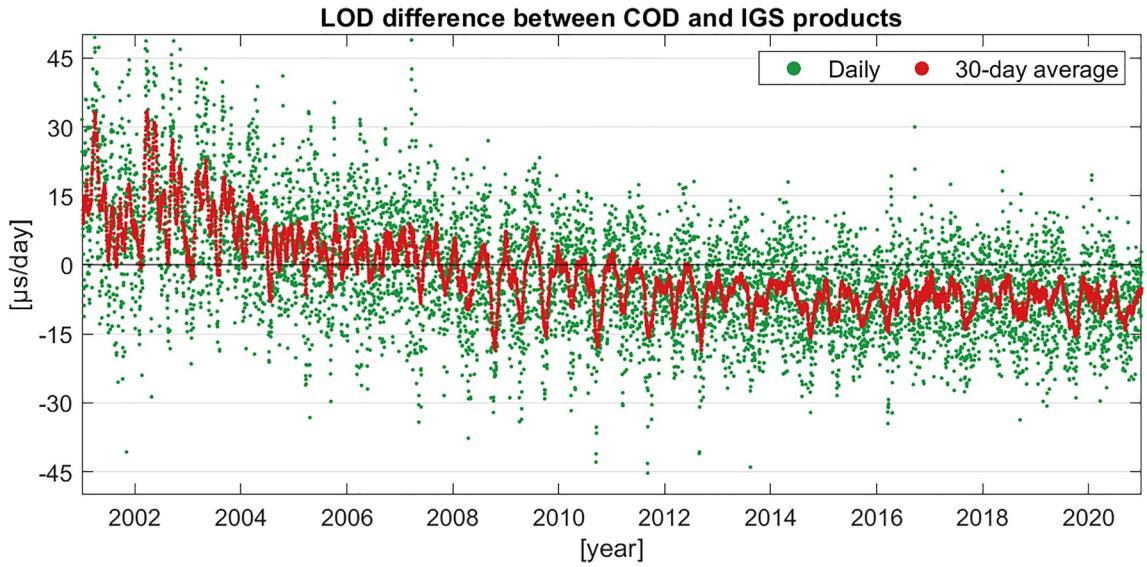

Figure 2. Length of Day (LOD) differences between Center for Orbit Determination in Europe (COD) and International Global Navigation Satellite System Service (IGS) products from 2001 to 2021.

2.4. Reference Solution

UT1-UTC estimates are usually evaluated by comparing to one of the IERS EOP products. In this study we use the IERS EOP 14C04 product (hereafter 14C04). Being a combination of different space geodetic techniques provided by various Analysis Centers (ACs), 14C04 includes UT1-UTC estimates of VLBI INT sessions and thus, cannot be seen as an independent reference. Note that IVS ACs ignore tropospheric gradients and do not apply GNSS–VLBI tropospheric ties in INT session analysis. Previous studies also showed that improvements can hardly be illustrated using 14C04 as a reference (Teke et al., 2015).

Moreover, UT1-UTC estimates can be indirectly evaluated via LOD obtained by differential quotients of UT1-UTC from successive sessions. GNSS provides very precise LOD estimates thanks to its continuous observations collected from a globally distributed network, and the GNSS LOD is commonly used to evaluate UT1-UTC indirectly (Böhm et al., 2010; Landskron & Böhm, 2019; Nilsson et al., 2017; Teke et al., 2015). GNSS LOD, however, is stable on short time scales only, but suffers from spurious drifts on longer time scales (Ray, 1996; Ray et al., 2005; Rebischung et al., 2016). Systematic biases can be reduced by optimizing satellite solar radiation pressure modeling (Zajdel et al., 2020), or adopting a longer data processing arc, for instance, using 3-day instead of 1-day arcs (Lutz et al., 2015). However, the instabilities can hardly be fully removed using GNSS-only observations.

We use three LOD products in the evaluation, including (a) 14C04 product, (b) IGS weekly combined product, and (c) CCOD 3-day solution (Noll, 2010). IGS LOD is a combination of several ACs, and long-term biases are removed using the IERS Bulletin A product, which makes it not a "pure" GNSS solution (Mireault et al., 1999; Rebischung et al., 2016). COD LOD product is determined using GNSS observations only, and hence, systematic biases still exist, as shown in Figure 2. For both IGS and COD products, we use the estimates of the IGS second reprocessing campaign before 2014 (Griffiths, 2018), and thereafter the operational product.

For comparison of both UT1-UTC and LOD, we first remove the effect of zonal tides of the reference product and then linearly interpolate to the middle epoch of an INT session. As LOD is not directly estimable in one INT session due to the short time, we use two consecutive sessions within 1.2 days to determine LOD, which refers to the middle of these two sessions. For each type of INT session, we calculate the UT1-UTC and LOD differences to reference products and evaluate the results using the weighted average (WAVG), weighted standard deviation (WSTD), and weighted root mean square (WRMS) of the differences.

21699356, 2022, 11, Downloaded from https://agupubs.onlinelibrary.wiley.com/doi/10.1029/2022JB025228 by Helmholtz-Zentrum Potsdam GFZ, Wiley Online Library on [28/11/2022]. See the Terms and Conditions (https://onlinelibrary.wiley.com/terms-and-conditions) on Wiley Online Library for rules of use; OA articles are governed by the applicable Creative Commons License

$$\mathrm{WAVG} = \frac{\sum_{i=1}^{n} \Delta x_i \cdot w_i}{\sum_{i=1}^{n} w_i}$$

$$\mathrm{WSTD} = \sqrt{\frac{\sum_{i=1}^{n} (\Delta x_i - \mathrm{WAVG})^2 \cdot w_i}{\sum_{i=1}^{n} w_i}} \tag{2}$$

$$\mathrm{WRMS} = \sqrt{\frac{\sum_{i=1}^{n} \Delta x_i{}^2 \cdot w_i}{\sum_{i=1}^{n} w_i}}$$

Δx_i is UT1-UTC (or LOD) difference of the ith estimate and w_i is the corresponding weight, derived from the formal error. We present all three statistics, but focus on the WSTD values for precision evaluation because the systematic bias might be caused by the reference product.

We do not consider sessions if (a) less than six observations are available, (b) the UT1-UTC difference compared to 14C04 is larger than 150 μs, or (c) the UT1-UTC difference is not within five times of the WRMS value. Note that if one session is considered as an outlier in one scenario, it is removed from all scenarios, so that we keep the identical sessions in different scenarios.

2.5. Linear Regression Analysis

To further quantify the impact of different tropospheric delay components on UT1-UTC, we perform the linear regression analysis of the UT1-UTC differences to the tropospheric parameter differences before and after applying tropospheric ties, specifically, between solution G0NT and solution G1AT. In solution G0NT tropospheric gradients are not estimated, that is, gradients are fixed to be zero. Such an investigation was also performed by Nilsson et al. (2011) and Teke et al. (2015), where the sum of east gradients at two VLBI radio telescopes was used to apply a simple regression analysis.

$$\Delta(\mathrm{UT1} - \mathrm{UTC}) = \alpha + \beta \cdot (\Delta \mathrm{GE}_1 + \Delta \mathrm{GE}_2) \tag{3}$$

$\Delta(\mathrm{UT1} - \mathrm{UTC})$ denotes the UT1-UTC difference between two solutions, $\Delta \mathrm{GE}_1$ and $\Delta \mathrm{GE}_2$ denote the corresponding east gradient differences at two VLBI radio telescopes, and (α, β) are the regression coefficients to be fitted.

Similarly, multiple linear regression is adopted for a type of INT session with nsta stations.

$$\Delta(\mathrm{UT1} - \mathrm{UTC}) = \sum_{i=1}^{\mathrm{nsta}} (a_i \cdot \Delta \mathrm{ZWD}_i + b_i \cdot \Delta \mathrm{GN}_i + c_i \cdot \Delta \mathrm{GE}_i) \tag{4}$$

$\Delta \mathrm{ZWD}_i$, $\Delta \mathrm{GN}_i$, and $\Delta \mathrm{GE}_i$ denote the differences of ZWD, north gradient, and east gradient at ith station, respectively, and (a_i, b_i, c_i) are the regression coefficients.

It is worth mentioning that the regression analysis presents the impact of tropospheric parameters from a statistical perspective, that is, the empirically fitted coefficients can better represent the real situation, which might differ from those determined in the theoretical analysis (such as investigating partial derivatives) due to the correlation between clocks, tropospheric parameters, and UT1-UTC in data processing, especially in the INT sessions with limited observation geometry.

3. Results and Discussions

In this section, we present the impact of tropospheric ties on the estimated UT1-UTC in different types of INT sessions, grouped by baseline geometry (see Section 2.1). The number of UT1-UTC and LOD for each type of INT sessions in Figures 3–8 is also given in Figure S1 in the Supporting Information. The regression analysis of all types is given at the end.

21699356, 2022, 11, Downloaded from https://agupubs.onlinelibrary.wiley.com/doi/10.1029/2022JB025228 by Helmholtz-Zentrum Potsdam GFZ, Wiley Online Library on [28/11/2022]. See the Terms and Conditions (https://onlinelibrary.wiley.com/terms-and-conditions) on Wiley Online Library for rules of use; OA articles are governed by the applicable Creative Commons License

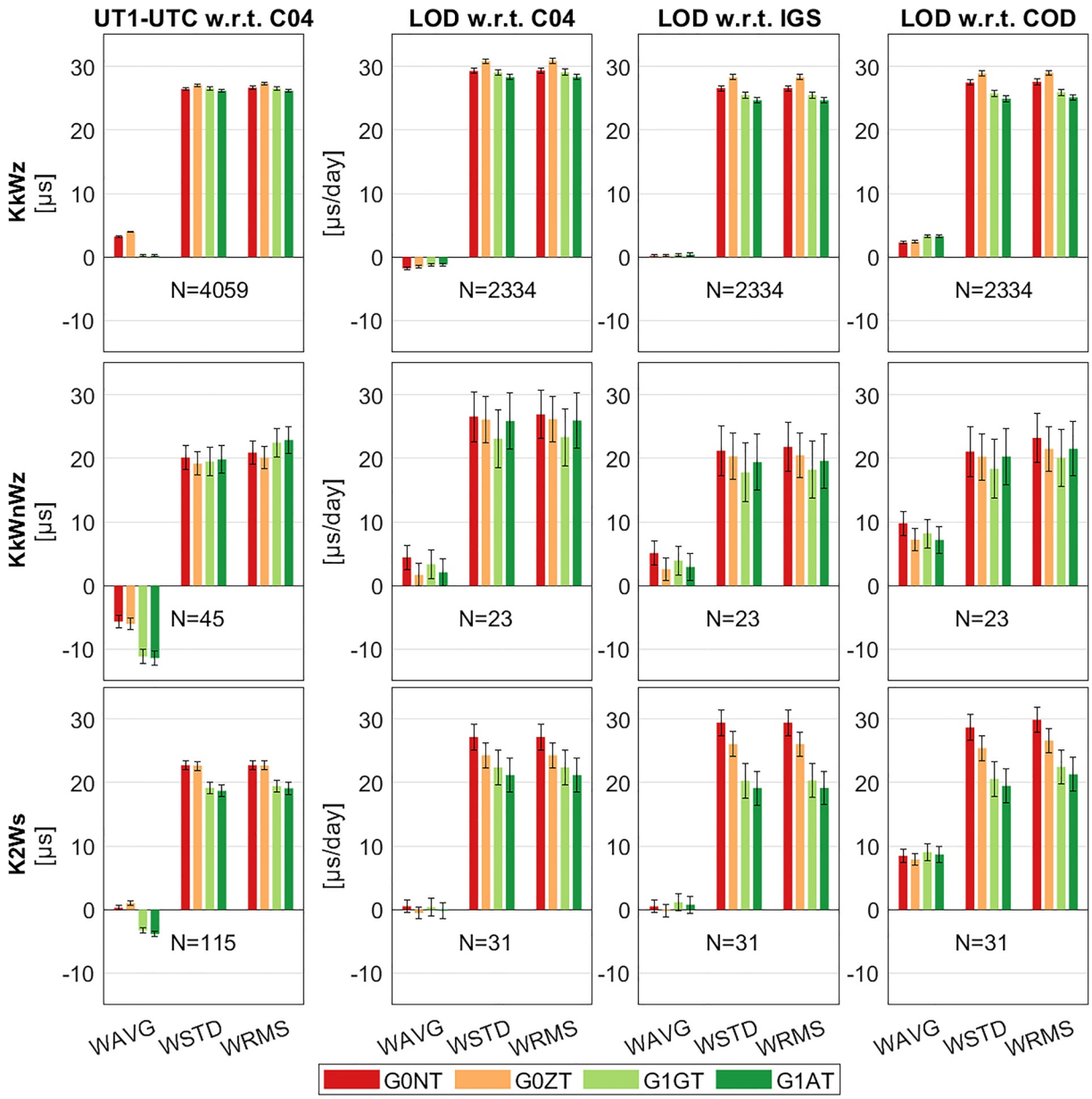

Figure 3. Agreement of Universal Time 1-Coordinate Universal Time (UT1-UTC) and Length of Day (LOD) of intensive (INT) sessions with baseline between Kokee Park and Wettzell radio telescopes. Left to right: UT1-UTC compared to 14C04, LOD compared to 14C04, LOD compared to International Global Navigation Satellite System Service (IGS) product, and LOD compared to Center for Orbit Determination in Europe (COD) product. Top to bottom: KkWz (INT1), KkWnWz (INT1), and K2Ws (VGOS-2). In each panel, the number of pairs is given, and the statistics include the weighted mean (WAVG), weighted standard deviation (WSTD), and weighted root mean square (WRMS). The error bars give the uncertainty of each statistic.

3.1. INT1 and VGOS-2: Sessions Between Kokee Park and Wettzell

Figure 3 presents the agreement of UT1-UTC and LOD for sessions between Kokee Park and Wettzell. Agreement of UT1-UTC to 14C04 is given in the left panels, including KkWz (INT1), KkWnWz (INT1), and K2Ws (VGOS-2) from top to bottom. On the one hand, applying gradient ties introduces systematic negative biases in UT1-UTC for all three types of sessions, as the WAVG value in solution G0NT is reduced from 3.2, –5.7, and 0.3 μs to 0.2, −11.4, and −3.3 μs in solution G1GT for KkWz, KkWnWz, and K2Ws sessions, respectively. On the other hand, the impact of gradient ties on WSTD is less than 1 μs for both KkWz and KkWnWz sessions, whereas the agreement of K2Ws sessions is improved by 15%, with the value reduced from 22.7 μs (G0NT) to

21699356, 2022, 11, Downloaded from https://agupubs.onlinelibrary.wiley.com/doi/10.1029/2022JB025228 by Helmholtz-Zentrum Potsdam GFZ, Wiley Online Library on [28/11/2022]. See the Terms and Conditions (https://onlinelibrary.wiley.com/terms-and-conditions) on Wiley Online Library for rules of use; OA articles are governed by the applicable Creative Commons License

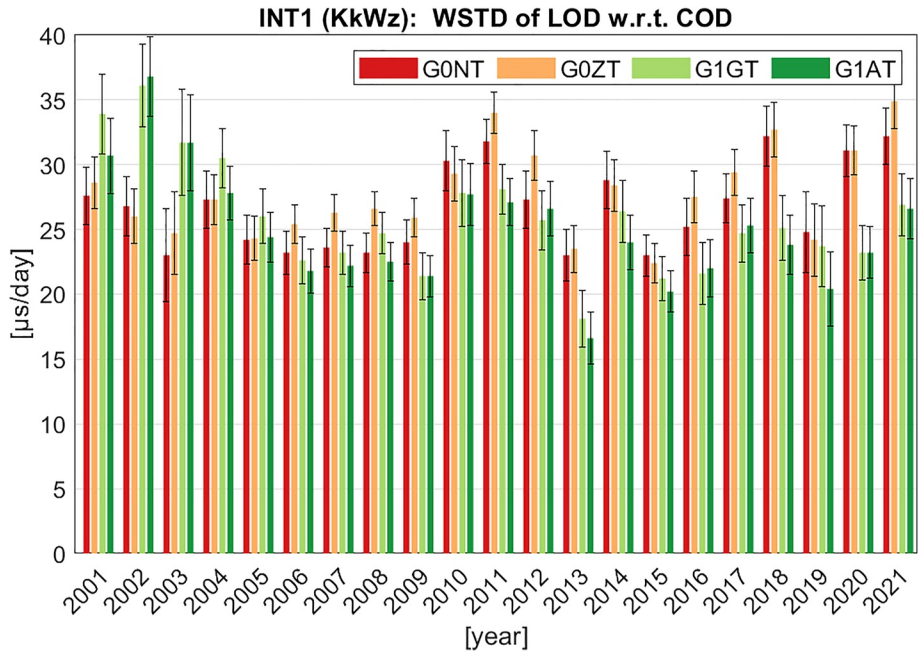

Figure 4. Yearly weighted standard deviation of Length of Day (LOD) differences between KkWz INT1 sessions and Center for Orbit Determination in Europe (COD) product. Uncertainties are given in error bars.

19.2 μs (G1GT). Applying ZTD ties has a small impact on UT1-UTC, which is usually negative since WSTD gets larger.

The impact of tropospheric ties on the agreement of LOD compared to 14C04 generally follows that of UT1-UTC. For both KkWnWz and KkWz sessions, applying ZTD ties only or gradient ties only, or applying them together usually causes a WSTD variation of less than 1 μs/day, which is relatively small as the WSTD is between 25 and 30 μs/day. However, we notice the exception of KkWnWz sessions when only gradient ties are applied, where the agreement is improved by 13%, with WSTD reduced from 26.5 μs/day (G0NT) to 23.1 μs/day (G1GT). The K2Ws sessions show a much better agreement to 14C04 LOD after applying tropospheric ties, with the WSTD value reduced from 27.1 μs/day (G0NT) to 24.3 μs/day by ZTD ties (G0ZT, 10%), 22.4 μs/day by gradient ties (G1GT, 17%), and 21.2 μs/day by ZTD and gradient ties together (G1AT, 22%).

The impact of tropospheric ties on LOD agreement to GNSS products is more significant. Applying ZTD ties degrades the agreement of KkWz sessions by 5%–6% in terms of WSTD, whereas applying gradient ties improves them by 4% and 7% when compared to IGS and COD products, respectively, and the corresponding improvement is 7% and 9% if both ZTD and gradient ties are applied. Both KkWnWz and K2Ws show a better LOD agreement to GNSS LOD after applying tropospheric ties. The KkWnWz sessions are improved by 5%–15%, depending on how tropospheric ties are applied. K2Ws sessions are improved by 12% and around 30% due to ZTD and gradient ties, respectively. The large LOD bias between INT sessions and the COD product is caused by the systematic biases of the latter (see Section 2.4), and will not be discussed in the following comparisons.

Noticing the long-term systematic time-varying LOD bias between COD and IGS products presented in Figure 2, we further investigate the yearly LOD agreement between KkWz sessions and the COD product. For each year we calculate the WSTD of LOD differences and apply the same outlier detection as described in Section 2.4. Figure 4 gives yearly WSTD statistics. On average, applying ZTD ties degrades the agreement by 1.2 μs/day (around 5%), whereas applying gradient ties and tropospheric ties (both ZTD and gradients) improves the agreement by 1.5 μs/day (6%) and 2.5 μs/day (10%), respectively. The uncertainty is within 0.4 μs/day. Moreover, the impact of tropospheric ties varies with time. Solution G1AT has a larger WSTD than solution G0NT before 2006, which could

21699356, 2022, 11, Downloaded from https://agupubs.onlinelibrary.wiley.com/doi/10.1029/2022JB025228 by Helmholtz-Zentrum Potsdam GFZ, Wiley Online Library on [28/11/2022]. See the Terms and Conditions (https://onlinelibrary.wiley.com/terms-and-conditions) on Wiley Online Library for rules of use; OA articles are governed by the applicable Creative Commons License

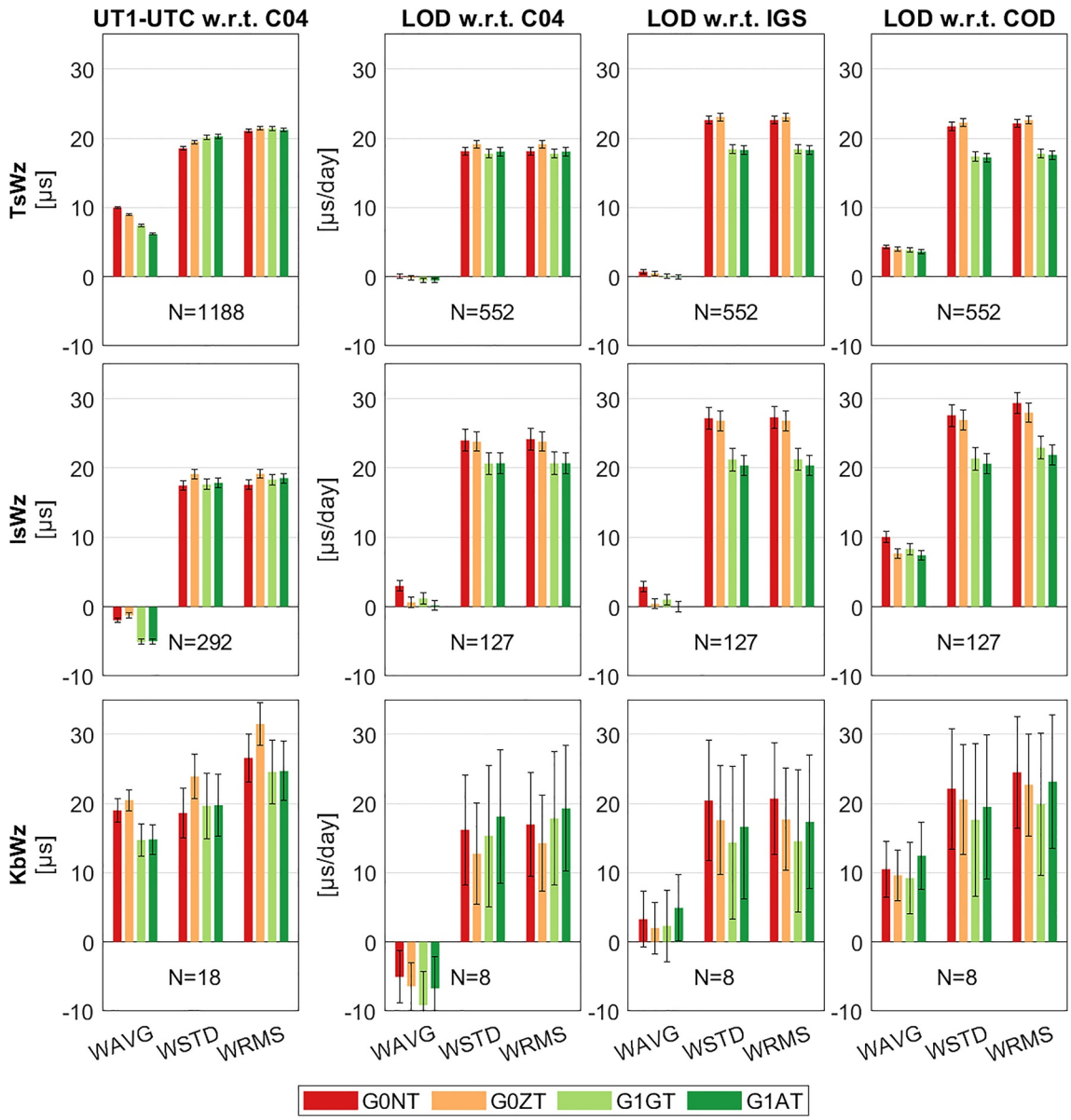

Figure 5. Agreement of Universal Time 1-Coordinate Universal Time (UT1-UTC) and Length of Day (LOD) of INT2 sessions including TsWz (2004–2014), IsWz (2016–2021), and KbWz (2008–2017). Left to right: UT1-UTC compared to 14C04, LOD compared to 14C04, LOD compared to International GNSS Service (IGS) product, and LOD compared to Center for Orbit Determination in Europe (COD) product.

be explained by (a) the precision of COD LOD keeps improving in this period, especially before 2004 due to the increase of stations in data processing (see Figures 1 and 4 of Rebischung et al. (2016)), (b) the quality of IGS orbits and clocks keeps improving in this period (see Figures 4 and 9 of Griffiths (2018)), indicating that GNSS tropospheric estimates are also improving in the first few years.

3.2. INT2 Sessions Between Japan and Wettzell

Figure 5 presents the agreement of UT1-UTC and LOD for INT2, mainly TsWz and IsWz sessions, and a few KbWz sessions. As shown in the left panels, the UT1-UTC agreement to 14C04 of neither TsWz nor IsWz sessions is improved when applying tropospheric ties, and the WSTD values are even slightly increased by less than 2 μs. The 18 KbWz sessions also show larger WSTD values after applying tropospheric ties. Similar to the

21699356, 2022, 11, Downloaded from https://agupubs.onlinelibrary.wiley.com/doi/10.1029/2022JB025228 by Helmholtz-Zentrum Potsdam GFZ, Wiley Online Library on [28/11/2022]. See the Terms and Conditions (https://onlinelibrary.wiley.com/terms-and-conditions) on Wiley Online Library for rules of use; OA articles are governed by the applicable Creative Commons License

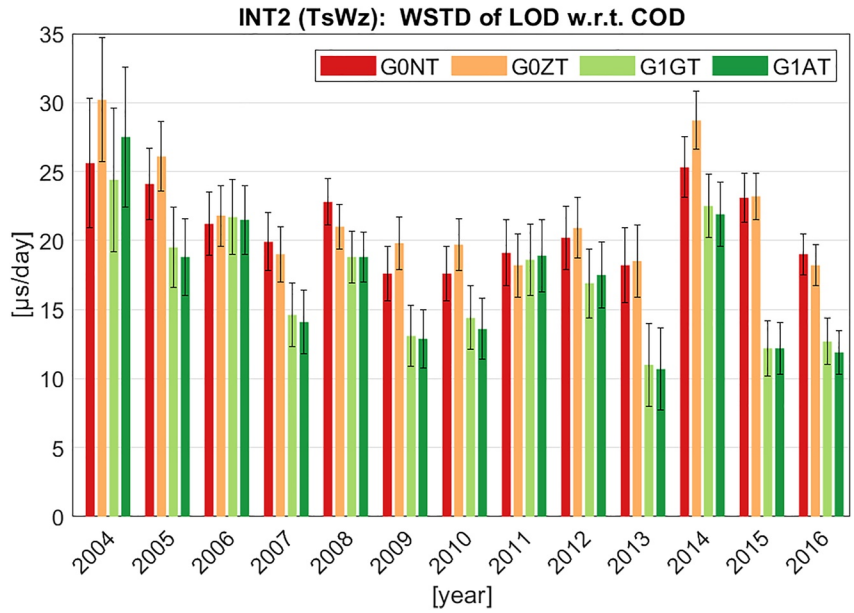

Figure 6. Yearly weighted standard deviation of Length of Day (LOD) differences between INT2 (TsWz) sessions and Center for Orbit Determination in Europe (COD) product. The uncertainty is given in the error bar.

sessions between radio telescopes in Kokee Park and those in Wettzell, applying gradient ties also introduces a negative systematic bias of −3 to −5 μs in UT1-UTC for TsWz, IsWz, and KbWz sessions.

When compared to the 14C04 LOD, the WSTD of TsWz sessions is around 18 μs/day, and applying tropospheric ties introduces a variation of less than 1 μs/day. The WSTD of IsWz sessions is around 24 μs/day, and applying gradient ties reduces the value to 20.7 μs/day, that is, 14% improvement. The KbWz sessions have a smaller WSTD if ZTD or gradient ties are applied, but a larger value when both ZTD and gradient ties are applied, despite the large uncertainty.

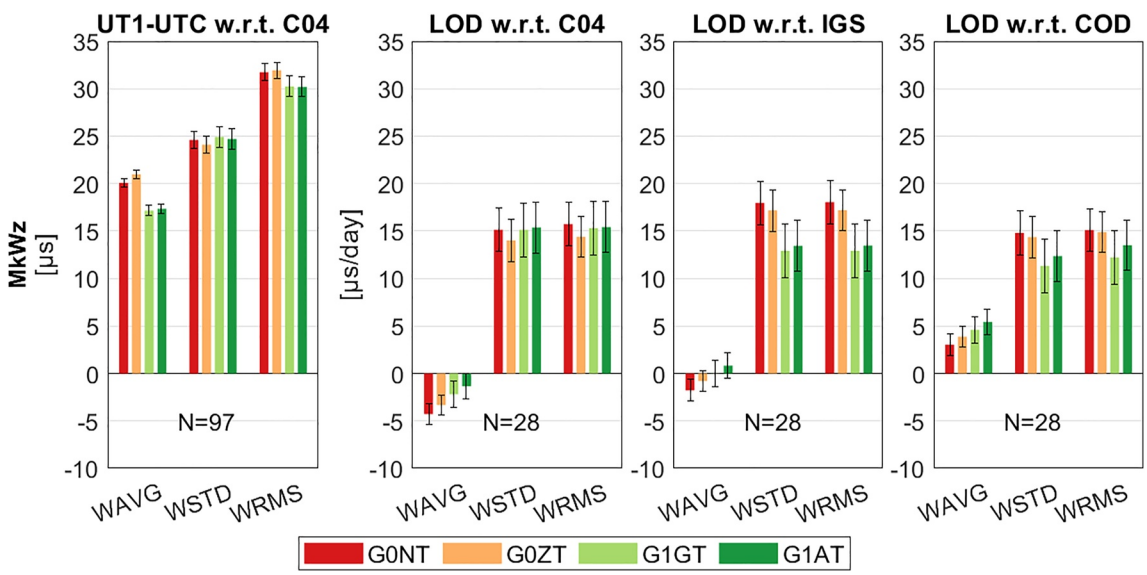

Figure 7. Results of Universal Time 1-Coordinate Universal Time (UT1-UTC) and Length of Day (LOD) for INT2 sessions between MK-VLBA and WETTZELL radio telescopes. Left to right: UT1-UTC compared to 14C04, LOD compared to 14C04, LOD compared to International GNSS Service (IGS) product, and LOD compared to Center for Orbit Determination in Europe (COD) product. The uncertainty is given in the error bar.

21699356, 2022, 11, Downloaded from https://agupubs.onlinelibrary.wiley.com/doi/10.1029/2022JB025228 by Helmholtz-Zentrum Potsdam GFZ, Wiley Online Library on [28/11/2022]. See the Terms and Conditions (https://onlinelibrary.wiley.com/terms-and-conditions) on Wiley Online Library for rules of use; OA articles are governed by the applicable Creative Commons License

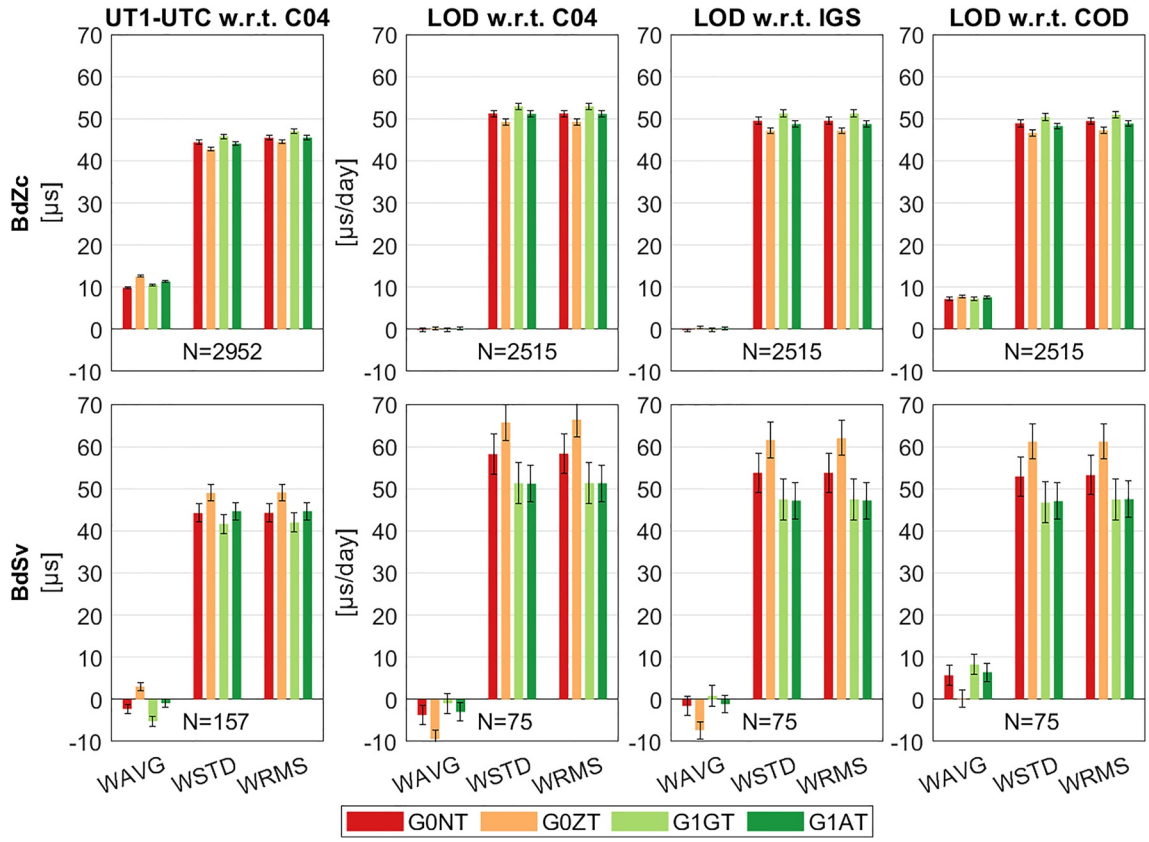

Figure 8. Results of Universal Time 1-Coordinate Universal Time (UT1-UTC) and Length of Day (LOD) for Russian BdZc (upper panels) and BdSv (lower panels) intensive sessions. Left to right: UT1-UTC compared to 14C04, LOD compared to 14C04, LOD compared to International GNSS Service (IGS) product, and LOD compared to Center for Orbit Determination in Europe (COD) product. The uncertainty is given in the error bar.

Comparing to GNSS LOD, both TsWz and IsWz sessions show significantly improved agreements by gradient ties by around 20% in terms of WSTD, while the impact of ZTD ties is within 1 μs/day, that is, deterioration for TsWz but improvement for IsWz sessions. The negative impact of ZTD ties for both KkWz and TsWz sessions was also reported by Nilsson et al. (2017). Moreover, TsWz sessions have a better agreement with GNSS LOD than the IsWz sessions by around 5 μs/day. As these two types of sessions are observed in different periods, that is, from 2004 to 2016 and after 2016, it is not easy to conclude which one performs better. The LOD of KbWz sessions is improved by tropospheric ties in general, even though the uncertainty is quite large.

Figure 6 gives the yearly LOD agreement between TsWz and the COD product from 2004 to 2016. Similar to the performance of KkWz sessions in Figure 4, TsWz sessions show a better agreement by tropospheric ties in most recent years, especially in 2013, 2015, and 2016 where the agreement improvement by gradient ties reaches up to 50%. The WAVG of all yearly WSTD values is reduced from 20.7 μs/day in solution G0NT to 16.1 μs/day in solution G1GT, and further to 15.8 μs/day in solution G1AT, with the uncertainty within 0.7 μs/day, again indicating the significantly improved agreement introduced by gradient ties.

As the COD LOD does not show a large between-year variation (see Figure 2) in the period 2016 to 2021, we do not present the yearly WSTD for IsWz sessions in this period.

3.3. INT2 Sessions Between MK-VLBA and WETTZELL

Figure 7 provides the UT1-UTC results of another INT2 type, that is, between VLBI radio telescope of MK-VLBA and that of WETTZELL. The UT1-UTC agreement to 14C04 is not significantly changed by tropospheric ties,

21699356, 2022, 11, Downloaded from https://agupubs.onlinelibrary.wiley.com/doi/10.1029/2022JB025228 by Helmholtz-Zentrum Potsdam GFZ, Wiley Online Library on [28/11/2022]. See the Terms and Conditions (https://onlinelibrary.wiley.com/terms-and-conditions) on Wiley Online Library for rules of use; OA articles are governed by the applicable Creative Commons License

21699356, 2022, 11, Downloaded from https://agupubs.onlinelibrary.wiley.com/doi/10.1029/2022JB025228 by Helmholtz-Zentrum Potsdam GFZ, Wiley Online Library on [28/11/2022]. See the Terms and Conditions (https://onlinelibrary.wiley.com/terms-and-conditions) on Wiley Online Library for rules of use; OA articles are governed by the applicable Creative Commons License

and the STD value is around 25 μs. However, the MkWz sessions show a large systematic discrepancy to 14C04, with the WAVG value of 20 μs in solution G0NT. Schartner et al. (2022) reported similar biases (10–20 μs) in the comparison of IVS ACs to 14C04 from 2020 to August 2021, and the corresponding STD values vary between 25 and 30 μs. Applying gradient ties introduces a negative systematic variation of around 3 μs in WAVG, which reduces the systematic bias to around 17 μs.

The LOD agreement with 14C04 is 15.1 μs/day in terms of WSTD, and applying ZTD or gradient ties has a small impact of less than 1 μs/day. In contrast, the impact of gradient ties is significantly beneficial when compared to GNSS LOD, and the agreement to IGS and COD products of G1GT to G0NT is improved by 28% and 24%, respectively. The impact of ZTD ties is rather small.

3.4. Russian INT Sessions Between Badary, Svetloe, and Zelenchukskaya

Figure 8 gives the results of UT1-UTC and LOD for RuI, including both BdZc (upper panels) and SvZc sessions (lower panels). The UT1-UTC agreement of these two types of sessions with 14C04 is around 45 μs, which is larger than that of IVS sessions (around 20–30 μs). This could be attributed to the relatively short baselines of these RuI. For BdZc sessions, applying ZTD ties improves the UT1-UTC agreement to 14C04 slightly, whereas applying gradient ties does the opposite, despite the small variation of 2 μs (less than 4%). The BdSv sessions show a deteriorated agreement by ZTD ties and improved one by gradient ties, within a magnitude of 3–4 μs.

Inspecting the LOD agreement, the WSTD of BdZc sessions is around 50 μs/day with respect to both 14C04 and GNSS products, and applying tropospheric ties has a small impact as the variations are less than 2–3 μs/day. The BdSv sessions show a worse LOD agreement than the BdZc sessions when compared to the 14C04 product as the WSTD is around 58 μs/day. Despite the large uncertainty, applying ZTD and gradient ties causes deteriorated and improved agreements of 12%, respectively, which are demonstrated in the LOD comparisons with 14C04, IGS, and COD LOD products. Nevertheless, applying ZTD and gradient ties together improves the LOD agreement of BdSv sessions to COD product by 20%, as the WSTD is reduced from 52.1 μs/day (G0NT) to 41.9 μs/day (G1AT), with an uncertainty of around 4 μs/day.

3.5. Regression Analysis

In this section, we present the regression analysis results of the UT1-UTC differences to the tropospheric delay differences between solution G0NT and solution G1AT, that is, the solution with neither tropospheric gradients nor tropospheric ties, and that with both ZTD and gradient ties.

An illustration of the KkWz sessions between Kokee Park and Wettzell is presented in Figure 9. Neither zenith delays nor north gradients introduce systematic impact since the regression coefficients are within 3 μs/mm. Considering that tropospheric gradients are usually less than 1 mm, this effect is negligible. However, UT1-UTC is largely affected by east gradients, and a 1 mm east gradient bias at Kokee Park or Wettzell causes a UT1-UTC change of 11–12 μs. Similar regression analysis was also presented before, such as 15 μs/mm by Böhm and Schuh (2007), 10–12 μs/mm by Nilsson et al. (2011), and 12.9 μs/mm by Teke et al. (2015), even though they fitted UT1-UTC differences as a function of the sum of east gradients at both stations. Moreover, both the single and multiple regression analyses in Figure 9 have comparable fitted coefficients, validating each other.

Figure 10 presents the regression analysis of the K2Ws (VGOS-2) sessions, sharing the same baseline geometry with KkWz sessions. Similar to KkWz sessions, the east gradients at both Kokee Park and Wettzell play a greater role in UT1-UTC estimates, and neither zenith delays nor north gradients introduce any systematic biases. The regression coefficient for the east gradient at Kokee Park (12.6 μs/mm) is comparable to that in KkWz sessions. However, the coefficient at Wettzell (25.1 μs/mm) is larger by a factor of two than that in KkWz sessions. The fitted coefficients agree well between the single and multiple regression analyses.

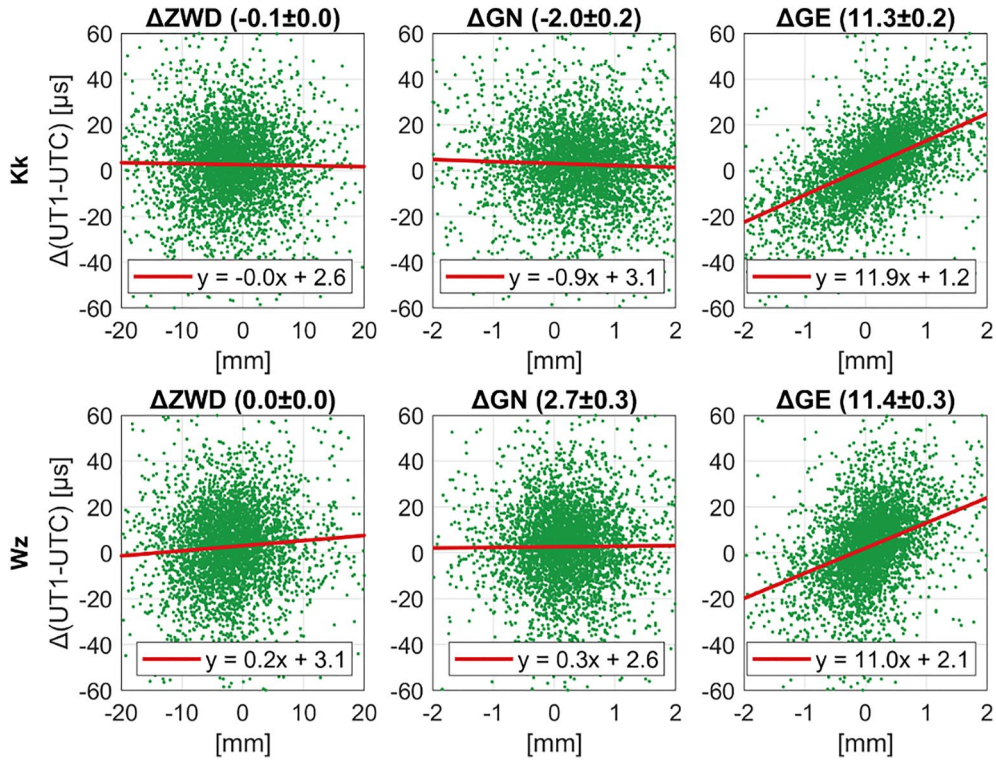

Figure 9. Linear regression analysis of Universal Time 1-Coordinate Universal Time (UT1-UTC) differences to tropospheric parameter differences between solution G0NT and G1AT for the KkWz (INT1) sessions, at KOKEE (upper panels) and WETTZELL (lower panels) radio telescopes. Left to right: analysis of ZWD, north gradient, and east gradient. The simple regression analysis is shown as the red line in each subplot, and the multiple regression analysis coefficient and uncertainty for each tropospheric delay component are given in the title of the corresponding subplot.

Noticing that the contribution of east gradient at Wettzell to UT1-UTC is larger in K2Ws sessions than in KkWz sessions by a factor of two, we further investigate the observation geometry of these two types of sessions. Figure 11 depicts the distribution of observations at each radio telescope in KkWz and K2Ws sessions in 2021.

For K2Ws, the observations in the east direction account for 70% and 28% at KOKEE12M and WETTZ13S, respectively; whereas for KkWz the corresponding number at KOKEE and WETTZELL is 58% and 41%. The observation gap of K2Ws sessions is caused by the blockage of the sky at KOKEE12M by the KOKEE 20 m radio telescope, as the latter is located in the northwest, around 30 m away and 8 m higher (Niell et al., 2021). For all INT1 sessions from 2001 to 2021, the east-west distribution is more homogeneous, that is, 54% and 45% in east direction for KOKEE and WETTZELL, respectively.

Table 3 summarizes the linear regression coefficients for INT sessions investigated in this study. For KkWnWz sessions with two radio telescopes at Wettzell, it is not possible to fit the coefficients of tropospheric gradients for both WETTZ13N and WETTZELL radio telescopes simultaneously, as they have the same tropospheric gradient variations between solution G0NT and G1AT. We thus exclude WETTZELL in the regression analysis. Similar to the KkWz and K2Ws sessions, it is still the east gradient that has a larger impact on UT1-UTC.

Unlike INT1 sessions between Kokee Park and Wettzell, north gradients at stations of INT2 sessions between Japan and Wettzell also introduce a systematic bias to UT1-UTC estimates. The UT1-UTC differences caused by 1 mm north gradient in Tsukuba or Ishioka is 4–5 μs, and that in Wettzell is −5 to −7 μs. The impact of east gradients on UT1-UTC is smaller for INT2 sessions than that for INT1 sessions, as the regression coefficients are around 7 μs/mm for INT2 sessions, except for the WETTZELL radio telescope in IsWz sessions. One possible reason for the different sensitivities to north gradients in Japan-Wettzell sessions is the baseline geometry: the east-west extension of Kokee-Wettzell baseline is larger (173°) than that of Japan-Wettzell baseline (127°), and thus the observation geometry is not the same. The large uncertainty of coefficients at KbWz sessions is caused by the limited number of sessions, 18 in total. Sharing a similar baseline geometry, MkWz sessions have

21699356, 2022, 11, Downloaded from https://agupubs.onlinelibrary.wiley.com/doi/10.1029/2022JB025228 by Helmholtz-Zentrum Potsdam GFZ, Wiley Online Library on [28/11/2022]. See the Terms and Conditions (https://onlinelibrary.wiley.com/terms-and-conditions) on Wiley Online Library for rules of use; OA articles are governed by the applicable Creative Commons License

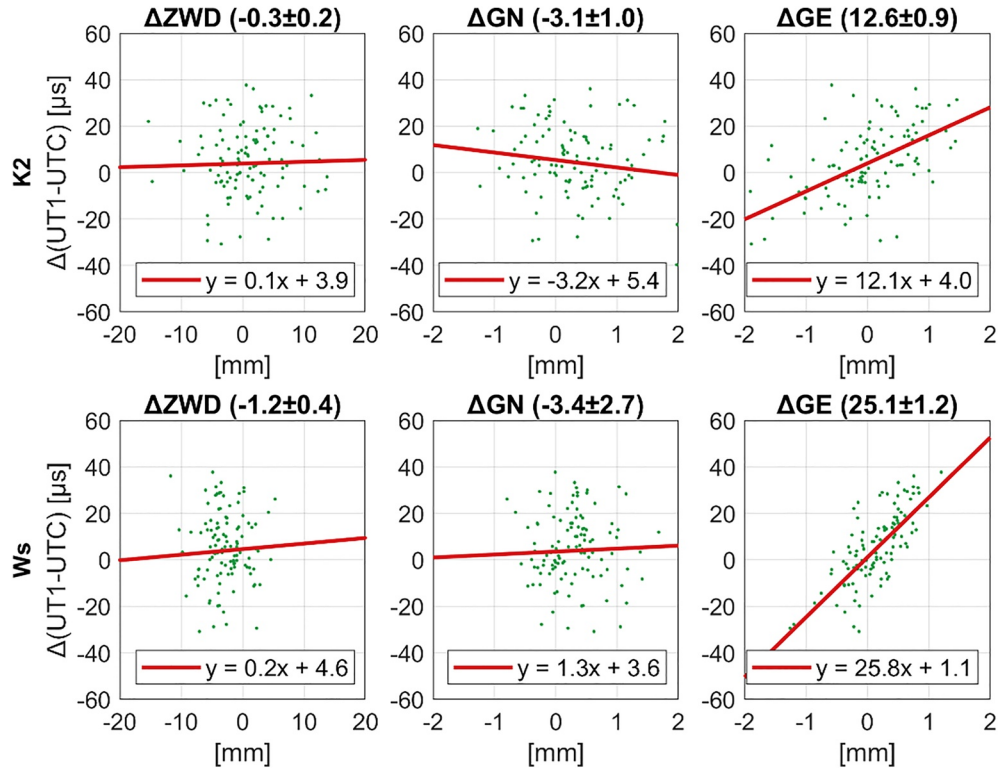

Figure 10. Linear regression analysis of Universal Time 1-Coordinate Universal Time (UT1-UTC) differences to tropospheric parameter differences between solution G0NT and G1AT for K2Ws (VGOS-2) sessions at KOKEE12M (upper panels) and WETTZ13S (lower panels) radio telescopes. Left to right: analysis of ZWD, north gradient, and east gradient. The simple regression analysis is shown as the red line in each subplot, and the multiple regression analysis coefficient and uncertainty for each tropospheric delay component are given in the title of the corresponding subplot.

comparable fitted coefficients with KkWz sessions. The RuI are more affected by the north gradient than the east one. For both BdZc and BdSv sessions, 1 mm north gradient at Badary leads to a bias in UT1-UTC of around 14 μs, and that at the second station introduces a negative bias with comparable magnitude.

4. Conclusions and Perspective

We investigate the impact of tropospheric ties between GNSS and VLBI co-located stations on UT1-UTC estimates in VLBI intensive sessions. Different types of INT sessions from 2001 to 2021 are analyzed, including those between Hawaii and Germany (INT1, INT2, and VGOS-2), between Japan and Germany (INT2), and RuI. A rigorous combination of GNSS and VLBI techniques on the observation level is performed, which assures the best consistency between the two techniques and is most suited to exploit the benefits of tropospheric ties.

Applying tropospheric ties improves the UT1-UTC estimates of INT1 (KkWz), INT2 (TsWz, IsWz, and MkWz), and VGOS-2 (K2Ws) sessions, but not of the RuI. However, the improvement can hardly be demonstrated if the IERS EOP 14C04 product is used as a reference, as only the K2Ws sessions show an improved agreement of 15%. The improvement is more significant when an indirect comparison to GNSS LOD is performed, as KkWz, TsWz, IsWz, MkWz, and K2Ws sessions are improved by 9%, 21%, 25%, 16%, and 32%, respectively, in terms of the WSTD agreement with COD LOD. The major contribution comes from tropospheric gradient ties, whereas applying only ZTD ties introduces a marginal improvement or even a deterioration, such as in KkWz and TsWz sessions. Applying tropospheric ties improves the LOD agreement with COD LOD for both KkWz and TsWz sessions after 2006, especially in the most recent years, whereas before 2006 the agreement is degraded, potentially caused by the relatively bad quality of GNSS products. Moreover, a systematic bias of −3 to −5 μs in UT1-UTC is introduced by gradient ties for the IVS INT sessions. The impact of tropospheric ties is quite small for the majority of RuI, that is, the BdZc sessions, whereas BdSv sessions are improved by 20%.

21699356, 2022, 11, Downloaded from https://agupubs.onlinelibrary.wiley.com/doi/10.1029/2022JB025228 by Helmholtz-Zentrum Potsdam GFZ, Wiley Online Library on [28/11/2022]. See the Terms and Conditions (https://onlinelibrary.wiley.com/terms-and-conditions) on Wiley Online Library for rules of use; OA articles are governed by the applicable Creative Commons License

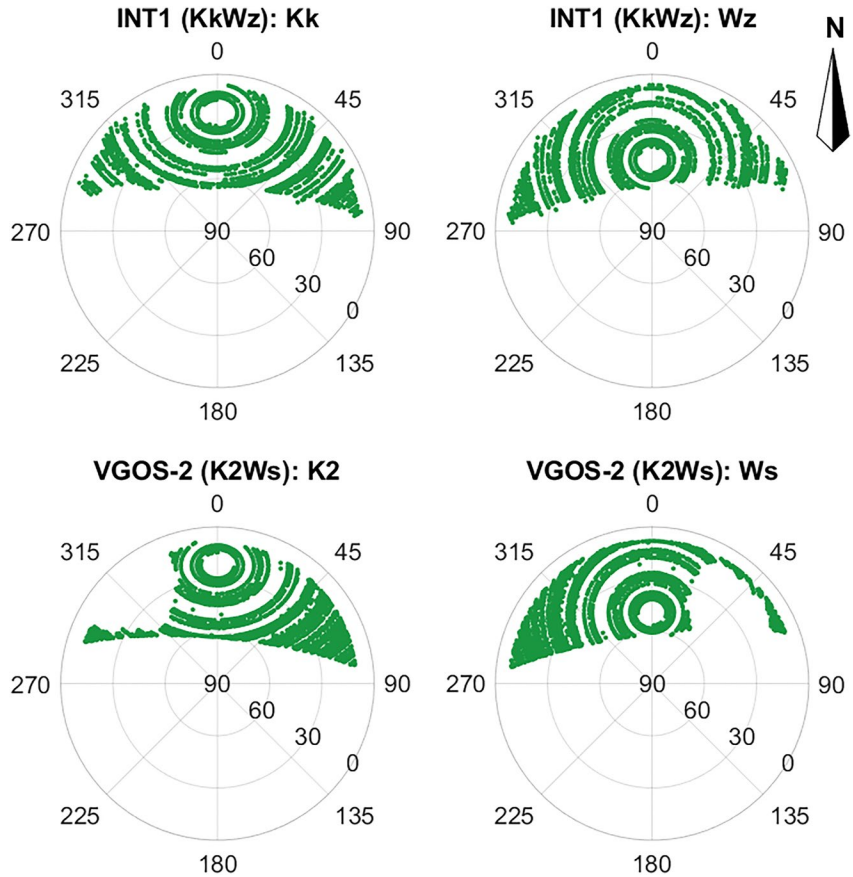

Figure 11. Distribution of observations for KkWz INT1 (upper panels) and K2Ws VGOS-2 (lower panels) sessions in 2021. Two Very Long Baseline Interferometry radio telescopes in Kokee Park (KOKEE and KOKEE12M in the left panels) and two in Wettzell (WETTZELL and WETTZ13S in the right panels).

Multiple regression analysis shows that for sessions between Kokee Park and Wettzell, the east gradient introduces a systematic bias in UT1-UTC estimates whereas the impact of ZTD and north gradients is negligible. Moreover, despite sharing the identical baseline geometry, K2Ws (VGOS-2) sessions are more sensitive to the east gradient at Wettzell than KkWz (INT1) sessions by a factor of two. For sessions between Japan and Germany,

Table 3
Linear Regression Coefficients of the Universal Time 1-Coordinate Universal Time (UT1-UTC) Differences to Tropospheric Parameter Differences Between Solution G0NT and G1AT

INT	ZWD [μs/mm]	GN [μs/mm]	GE [μs/mm]
KkWz	−0.1 ± 0.0, 0.1 ± 0.0	2.0 ± 0.2, 2.7 ± 0.3	11.3 ± 0.2, 11.4 ± 0.3
K2Ws	−0.3 ± 0.2, −1.2 ± 0.4	−3.1 ± 0.9, −3.4 ± 2.7	12.6 ± 0.9, 25.1 ± 1.2
KkWn(Wz)	−0.7 ± 0.2, −0.0 ± 0.1	−2.0 ± 1.6, −0.9 ± 1.6	9.0 ± 1.9, 19.8 ± 4.3
TsWz	0.6 ± 0.0, −0.6 ± 0.1	5.5 ± 0.3, −7.4 ± 0.4	7.8 ± 0.3, 7.3 ± 0.4
IsWz	0.5 ± 0.1, −0.1 ± 0.1	4.3 ± 0.6, −5.2 ± 0.8	7.4 ± 0.6, 4.5 ± 0.9
KbWz	0.2 ± 0.4, −0.5 ± 0.9	6.1 ± 1.9, 7.4 ± 7.1	8.7 ± 1.9, 17.9 ± 4.4
MkWz	0.0 ± 0.1, −0.3 ± 0.2	−2.8 ± 0.9, 1.6 ± 1.6	11.1 ± 0.8, 16.6 ± 0.8
BdZc	0.7 ± 0.0, −0.6 ± 0.0	14.4 ± 0.4, −11.0 ± 0.3	2.1 ± 0.4, 7.9 ± 0.3
BdSv	1.0 ± 0.2, −0.7 ± 0.2	14.3 ± 1.3, −14.6 ± 1.4	9.2 ± 1.7, 8.5 ± 2.2

Note. The fitted coefficient and uncertainty for different VLBI radio telescopes are separated by a comma. For KkWnWz sessions, only one VLBI radio telescope in Wettzell is used in the fitting.

21699356, 2022, 11, Downloaded from https://agupubs.onlinelibrary.wiley.com/doi/10.1029/2022JB025228 by Helmholtz-Zentrum Potsdam GFZ, Wiley Online Library on [28/11/2022]. See the Terms and Conditions (https://onlinelibrary.wiley.com/terms-and-conditions) on Wiley Online Library for rules of use; OA articles are governed by the applicable Creative Commons License

21699356, 2022, 11, Downloaded from https://agupubs.onlinelibrary.wiley.com/doi/10.1029/2022JB025228 by Helmholtz-Zentrum Potsdam GFZ, Wiley Online Library on [28/11/2022]. See the Terms and Conditions (https://onlinelibrary.wiley.com/terms-and-conditions) on Wiley Online Library for rules of use; OA articles are governed by the applicable Creative Commons License

east and north gradients both cause systematic biases. The north gradient plays a greater role in causing systematic biases than the east one for RuI. Therefore, for the scheduling of future VLBI intensive sessions, the impact of tropospheric horizontal gradients should be considered, in addition to other factors such as the baseline geometry (Schartner et al., 2021, 2022). If GNSS co-location stations are not available or applying tropospheric ties is not feasible, then VLBI radio telescopes located in high tropospheric gradient region should be avoided.

Thus, a combination of GNSS and VLBI on the observation level is recommended. This procedure should be investigated for the further IVS operational processing and reprocessing, or at least external tropospheric delays from GNSS should be utilized. As the current IERS EOP 14C04 is not a proper reference to evaluate our results, this product still has space for further improvements. Ignoring the tropospheric tie biases related to instrument might be a reason for the deterioration after applying ZTD ties, and thus the long-term single-technique solutions should be performed using homogeneous strategies, and tropospheric tie biases should be carefully calibrated and applied in the integrated solution.

As we demonstrate that tropospheric ties can effectively improve the UT1-UTC in VLBI intensive sessions, applying additional ties, such as global ties (e.g., Hellmers et al., 2019), local ties, and clock ties (Hobiger & Otsubo, 2014) is expected to further improve the solutions. In this study, clock modeling strategies for GNSS and VLBI are different, and it is not possible to apply clock ties as common clocks are not available yet. Considering that GNSS has a much better observation geometry with more than six satellites tracked, it is possible to model clock as white noise and capture the high-frequency variations. Therefore, applying clock ties would potentially improve the VLBI estimates, and we will examine the impact of GNSS-VLBI clock ties in both intensive and 24-hr sessions in simulations in further studies.

Data Availability Statement

The GNSS from IGS and VLBI observations from IVS are available at CDDIS (Noll, 2010), the reference UT1-UTC is provided by IERS (https://www.iers.org/IERS/EN/DataProducts/EarthOrientationData/eop.html), the NWM-derived tropospheric delay products are provided by TU Wien (http://doi.org/10.17616/R3RD2H).

Acknowledgments
We would like to thank IGS and IVS for providing observations and products of GNSS and VLBI, IERS for providing EOP products, and TU Wien for providing tropospheric delay products. We would like to thank Dr. James M. Anderson for his support in converting vgosDB into NGSCARD format. We thank the associated editor Dr. Paul Tregoning and the anonymous reviewers for reviewing this manuscript and the insightful comments. Jungang Wang is funded by the Helmholtz OCPC Program (Grant ZD202121). Kyriakos Balidakis is funded by the Deutsche Forschungsgemeinschaft (DFG)—Project-ID 434617780—SFB 1464 (TerraQ). Open Access funding enabled and organized by Projekt DEAL.

References

Altamimi, Z., Rebischung, P., Métivier, L., & Collilieux, X. (2016). ITRF2014: A new release of the international terrestrial reference frame modeling nonlinear station motions. *Journal of Geophysical Research: Solid Earth*, *121*(8), 6109–6131. https://doi.org/10.1002/2016jb013098

Artz, T., Leek, J., Nothnagel, A., & Schumacher, M. (2012). VLBI intensive sessions revisited. In *Paper presented at IVS 2012 general meeting proceedings*, p. 276–280. http://ivscc.gsfc.nasa.gov/publications/gm2012/artz.pdf

Baver, K., & Gipson, J. (2020). Balancing source strength and sky coverage in IVS-INT01 scheduling. *Journal of Geodesy*, *94*(2), 18. https://doi.org/10.1007/s00190-020-01343-1

Bizouard, C., Lambert, S., Gattano, C., Becker, O., & Richard, J.-Y. (2018). The IERS EOP 14C04 solution for Earth orientation parameters consistent with ITRF 2014. *Journal of Geodesy*, *93*(5), 621–633. https://doi.org/10.1007/s00190-018-1186-3

Böckmann, S., Artz, T., Nothnagel, A., & Tesmer, V. (2010). International VLBI service for geodesy and astrometry: Earth orientation parameter combination methodology and quality of the combined products. *Journal of Geophysical Research*, *115*(B4), B04404. https://doi.org/10.1029/2009jb006465

Böhm, J., Hobiger, T., Ichikawa, R., Kondo, T., Koyama, Y., Pany, A., et al. (2010). Asymmetric tropospheric delays from numerical weather models for UT1 determination from VLBI Intensive sessions on the baseline Wettzell–Tsukuba. *Journal of Geodesy*, *84*(5), 319–325. https://doi.org/10.1007/s00190-010-0370-x

Böhm, J., & Schuh, H. (2007). Forecasting data of the troposphere used for IVS Intensive sessions. In *Paper presented at proceedings of the 18th European VLBI for geodesy and astrometry working meeting, Vienna*.

Charlot, P., Jacobs, C. S., Gordon, D., Lambert, S., de Witt, A., Böhm, J., et al. (2020). The third realization of the international celestial reference frame by very long baseline interferometry. *Astronomy & Astrophysics*, *644*, A159. https://doi.org/10.1051/0004-6361/202038368

Chen, G., & Herring, T. A. (1997). Effects of atmospheric azimuthal asymmetry on the analysis of space geodetic data. *Journal of Geophysical Research*, *102*(B9), 20489–20502. https://doi.org/10.1029/97jb01739

Diamantidis, P.-K., Kłopotek, G., & Haas, R. (2021). VLBI and GPS inter- and intra-technique combinations on the observation level for evaluation of TRF and EOP. *Earth Planets and Space*, *73*(1), 68. https://doi.org/10.1186/s40623-021-01389-1

Duan, P., & Huang, C. (2020). Intradecadal variations in length of day and their correspondence with geomagnetic jerks. *Nature Communications*, *11*(1), 2273. https://doi.org/10.1038/s41467-020-16109-8

Gambis, D., & Luzum, B. (2011). Earth rotation monitoring, UT1 determination and prediction. *Metrologia*, *48*(4), S165–S170. https://doi.org/10.1088/0026-1394/48/4/s06

Geng, J. H., Shi, C., Zhao, Q. L., Ge, M. R., & Liu, J. N. (2008). Integrated adjustment of LEO and GPS in precision orbit determination. In *Paper presented at VI Hotine-Marussi Symposium on theoretical and computational geodesy*. International Association of Geodesy Symposia, Springer. https://doi.org/10.1007/978-3-540-74584-6_20

Gipson, J., & Baver, K. (2015). Improvement of the IVS-INT01 sessions by source selection: Development and evaluation of the maximal source strategy. *Journal of Geodesy*, *90*(3), 287–303. https://doi.org/10.1007/s00190-015-0873-6

Griffiths, J. (2018). Combined orbits and clocks from IGS second reprocessing. *Journal of Geodesy*, *93*(2), 177–195. https://doi.org/10.1007/s00190-018-1149-8

Haas, R., Varenius, E., Matsumoto, S., & Schartner, M. (2021). Observing UT1-UTC with VGOS. *Earth Planets and Space*, *73*(1), 78. https://doi.org/10.1186/s40623-021-01396-2

He, L., Ge, M., Wang, J., Wickert, J., & Schuh, H. (2013). Experimental study on the precise orbit determination of the BeiDou navigation satellite system. *Sensors*, *13*(3), 2911–2928. https://doi.org/10.3390/s130302911

Heinkelmann, R., Böhm, J., Schuh, H., Bolotin, S., Engelhardt, G., MacMillan, D. S., et al. (2007). Combination of long time-series of troposphere zenith delays observed by VLBI. *Journal of Geodesy*, *81*(6–8), 483–501. https://doi.org/10.1007/s00190-007-0147-z

Hellmers, H., Thaller, D., Bloßfeld, M., Kehm, A., & Girdiuk, A. (2019). Combination of VLBI intensive sessions with GNSS for generating low latency Earth rotation parameters. *Advances in Geosciences*, *50*, 49–56. https://doi.org/10.5194/adgeo-50-49-2019

Hobiger, T., & Otsubo, T. (2014). Combination of GPS and VLBI on the observation level during CONT11—Common parameters, ties and inter-technique biases. *Journal of Geodesy*, *88*(11), 1017–1028. https://doi.org/10.1007/s00190-014-0740-x

Hobiger, T., Otsubo, T., Sekido, M., Gotoh, T., Kubooka, T., & Takiguchi, H. (2011). Fully automated VLBI analysis with c5++ for ultra-rapid determination of UT1. *Earth Planets and Space*, *62*(12), 933–937. https://doi.org/10.5047/eps.2010.11.008

Johnson, T. J., Luzum, B. J., & Ray, J. R. (2005). Improved near-term Earth rotation predictions using atmospheric angular momentum analysis and forecasts. *Journal of Geodynamics*, *39*(3), 209–221. https://doi.org/10.1016/j.jog.2004.10.004

Johnston, G., Riddell, A., & Hausler, G. (2017). The international GNSS Service. In P. J. G. Teunissen & O. Montenbruck (Eds.), *Springer handbook of global navigation satellite systems* (1st ed., pp. 967–982). Springer International Publishing. https://doi.org/10.1007/978-3-319-42928-1_33

Kalarus, M., Schuh, H., Kosek, W., Akyilmaz, O., Bizouard, C., Gambis, D., et al. (2010). Achievements of the Earth orientation parameters prediction comparison campaign. *Journal of Geodesy*, *84*(10), 587–596. https://doi.org/10.1007/s00190-010-0387-1

Kareinen, N., Hobiger, T., & Haas, R. (2015). Automated analysis of Kokee–Wettzell intensive VLBI sessions—Algorithms, results, and recommendations. *Earth Planets and Space*, *67*(1), 181. https://doi.org/10.1186/s40623-015-0340-x

Kareinen, N., Klopotek, G., Hobiger, T., & Haas, R. (2017). Identifying optimal tag-along station locations for improving VLBI Intensive sessions. *Earth Planets and Space*, *69*(1), 16. https://doi.org/10.1186/s40623-017-0601-y

Krügel, M., Thaller, D., Tesmer, V., Rothacher, M., Angermann, D., & Schmid, R. (2007). Tropospheric parameters: Combination studies based on homogeneous VLBI and GPS data. *Journal of Geodesy*, *81*(6–8), 515–527. https://doi.org/10.1007/s00190-006-0127-8

Landskron, D., & Böhm, J. (2017). VMF3/GPT3: Refined discrete and empirical troposphere mapping functions. *Journal of Geodesy*, *92*(4), 349–360. https://doi.org/10.1007/s00190-017-1066-2

Landskron, D., & Böhm, J. (2019). Improving dUT1 from VLBI intensive sessions with GRAD gradients and ray-traced delays. *Advances in Space Research*, *63*(11), 3429–3435. https://doi.org/10.1016/j.asr.2019.03.041

Liu, J., & Ge, M. (2003). PANDA software and its preliminary result of positioning and orbit determination. *Wuhan University Journal of Natural Sciences*, *8*(2), 603–609. https://doi.org/10.1007/BF02899825

Liu, Y., Ge, M., Shi, C., Lou, Y., Wickert, J., & Schuh, H. (2016). Improving integer ambiguity resolution for GLONASS precise orbit determination. *Journal of Geodesy*, *90*(8), 715–726. https://doi.org/10.1007/s00190-016-0904-y

Lutz, S., Meindl, M., Steigenberger, P., Beutler, G., Sośnica, K., Schaer, S., et al. (2015). Impact of the arc length on GNSS analysis results. *Journal of Geodesy*, *90*(4), 365–378. https://doi.org/10.1007/s00190-015-0878-1

Luzum, B., & Nothnagel, A. (2010). Improved UT1 predictions through low-latency VLBI observations. *Journal of Geodesy*, *84*(6), 399–402. https://doi.org/10.1007/s00190-010-0372-8

Malkin, Z. (2011). The impact of celestial pole offset modelling on VLBI UT1 intensive results. *Journal of Geodesy*, *85*(9), 617–622. https://doi.org/10.1007/s00190-011-0468-9

Malkin, Z. (2013). Impact of seasonal station motions on VLBI UT1 intensives results. *Journal of Geodesy*, *87*(6), 505–514. https://doi.org/10.1007/s00190-013-0624-5

Mikschi, M., Böhm, J., & Schartner, M. (2021). Unconstrained estimation of VLBI global observing system station coordinates. *Advances in Geosciences*, *55*, 23–31. https://doi.org/10.5194/adgeo-55-23-2021

Mireault, Y., Kouba, J., & Ray, J. (1999). IGS Earth rotation parameters. *GPS Solutions*, *3*(1), 59–72. https://doi.org/10.1007/pl00012781

Nafisi, V., Madzak, M., Böhm, J., Ardalan, A. A., & Schuh, H. (2012). Ray-traced tropospheric delays in VLBI analysis. *Radio Science*, *47*(2). https://doi.org/10.1029/2011rs004918

Niedzielski, T., & Kosek, W. (2007). Prediction of UT1–UTC, LOD and AAM χ3 by combination of least-squares and multivariate stochastic methods. *Journal of Geodesy*, *82*(2), 83–92. https://doi.org/10.1007/s00190-007-0158-9

Niell, A., Barrett, J., Burns, A., Cappallo, R., Corey, B., Derome, M., et al. (2018). Demonstration of a broadband very long baseline interferometer system: A new instrument for high-precision space geodesy. *Radio Science*, *53*(10), 1269–1291. https://doi.org/10.1029/2018rs006617

Niell, A. E., Barrett, J. P., Cappallo, R. J., Corey, B. E., Elosegui, P., Mondal, D., et al. (2021). VLBI measurement of the vector baseline between geodetic antennas at Kokee Park Geophysical Observatory, Hawaii. *Journal of Geodesy*, *95*(6), 65. https://doi.org/10.1007/s00190-021-01505-9

Nilsson, T., Böhm, J., & Schuh, H. (2011). Universal time from VLBI single-baseline observations during CONT08. *Journal of Geodesy*, *85*(7), 415–423. https://doi.org/10.1007/s00190-010-0436-9

Nilsson, T., Soja, B., Balidakis, K., Karbon, M., Heinkelmann, R., Deng, Z., & Schuh, H. (2017). Improving the modeling of the atmospheric delay in the data analysis of the Intensive VLBI sessions and the impact on the UT1 estimates. *Journal of Geodesy*, *91*(7), 857–866. https://doi.org/10.1007/s00190-016-0985-7

Noll, C. E. (2010). The crustal dynamics data information system: A resource to support scientific analysis using space geodesy. *Advances in Space Research*, *45*(12), 1421–1440. https://doi.org/10.1016/j.asr.2010.01.018

Nothnagel, A., Artz, T., Behrend, D., & Malkin, Z. (2016). International VLBI service for geodesy and astrometry. *Journal of Geodesy*, *91*(7), 711–721. https://doi.org/10.1007/s00190-016-0950-5

Nothnagel, A., & Schnell, D. (2008). The impact of errors in polar motion and nutation on UT1 determinations from VLBI Intensive observations. *Journal of Geodesy*, *82*(12), 863–869. https://doi.org/10.1007/s00190-008-0212-2

Penna, N. T., Morales Maqueda, M. A., Martin, I., Guo, J., & Foden, P. R. (2018). Sea surface height measurement using a GNSS wave glider. *Geophysical Research Letters*, *45*(11), 5609–5616. https://doi.org/10.1029/2018gl077950

Petit, G., & Luzum, B. (2010). IERS conventions (2010). (IERS Technical Note No. 36)Rep. https://iers-conventions.obspm.fr/content/tn36.pdf

Petrachenko, W. T., Niell, A. E., Corey, B. E., Behrend, D., Schuh, H., & Wresnik, J. (2012). VLBI2010: Next generation VLBI system for geodesy and astrometry. *Geodesy for Planet Earth*, *136*, 999–1005. https://doi.org/10.1007/978-3-642-20338-1_125

Puente, V., Azcue, E., Gomez-Espada, Y., & Garcia-Espada, S. (2021). Comparison of common VLBI and GNSS estimates in CONT17 campaign. *Journal of Geodesy*, *95*(11), 120. https://doi.org/10.1007/s00190-021-01565-x

21699356, 2022, 11, Downloaded from https://agupubs.onlinelibrary.wiley.com/doi/10.1029/2022JB025228 by Helmholtz-Zentrum Potsdam GFZ, Wiley Online Library on [28/11/2022]. See the Terms and Conditions (https://onlinelibrary.wiley.com/terms-and-conditions) on Wiley Online Library for rules of use; OA articles are governed by the applicable Creative Commons License

Ray, J., Kouba, J., & Altamimi, Z. (2005). Is there utility in rigorous combinations of VLBI and GPS Earth orientation parameters? *Journal of Geodesy*, *79*(9), 505–511. https://doi.org/10.1007/s00190-005-0007-7

Ray, J. R. (1996). Measurements of length of day using the global positioning system. *Journal of Geophysical Research*, *101*(B9), 20141–20149. https://doi.org/10.1029/96jb01889

Rebischung, P., Altamimi, Z., Ray, J., & Garayt, B. (2016). The IGS contribution to ITRF2014. *Journal of Geodesy*, *90*(7), 611–630. https://doi.org/10.1007/s00190-016-0897-6

Rebischung, P., & Schmid, R. (2016). IGS14/igs14. atx: A new framework for the IGS products. In *Paper presented at AGU fall meeting 2016*. https://mediatum.ub.tum.de/doc/1341338/file.pdf

Robertson, D. S., Carter, W. E., Campbell, J., & Schuh, H. (1985). Daily Earth rotation determinations from IRIS very long baseline interferometry. *Nature*, *316*(6027), 424–427. https://doi.org/10.1038/316424a0

Schartner, M., Kern, L., Nothnagel, A., Bohm, J., & Soja, B. (2021). Optimal VLBI baseline geometry for UT1-UTC Intensive observations. *Journal of Geodesy*, *95*(7), 75. https://doi.org/10.1007/s00190-021-01530-8

Schartner, M., Plötz, C., & Soja, B. (2022). Improvements and comparison of VLBI INT2 and INT3 session performance. *Journal of Geodesy*, *96*(4), 26. https://doi.org/10.1007/s00190-022-01621-0

Schuh, H., Heinkelmann, R., Beyerle, G., Anderson, J. M., Balidakis, K., Belda, S., et al. (2021). The Potsdam open source radio interferometry tool (PORT). *Publications of the Astronomical Society of the Pacific*, *133*(1028), 104503. https://doi.org/10.1088/1538-3873/ac299c

Sekido, M., Takiguchi, H., Koyama, Y., Kondo, T., Haas, R., Wagner, J., et al. (2008). Ultra-rapid UT1 measurement by e-VLBI. *Earth Planets and Space*, *60*(8), 865–870. https://doi.org/10.1186/bf03352838

Shuygina, N., Ivanov, D., Ipatov, A., Gayazov, I., Marshalov, D., Melnikov, A., et al. (2019). Russian VLBI network "Quasar": Current status and outlook. *Geodesy and Geodynamics*, *10*(2), 150–156. https://doi.org/10.1016/j.geog.2018.09.008

Soja, B., Nilsson, T., Karbon, M., Zus, F., Dick, G., Deng, Z., et al. (2015). Tropospheric delay determination by Kalman filtering VLBI data. *Earth Planets and Space*, *67*(1), 144. https://doi.org/10.1186/s40623-015-0293-0

Teke, K., Böhm, J., Madzak, M., Kwak, Y., & Steigenberger, P. (2015). GNSS zenith delays and gradients in the analysis of VLBI Intensive sessions. *Advances in Space Research*, *56*(8), 1667–1676. https://doi.org/10.1016/j.asr.2015.07.032

Teke, K., Böhm, J., Nilsson, T., Schuh, H., Steigenberger, P., Dach, R., et al. (2011). Multi-technique comparison of troposphere zenith delays and gradients during CONT08. *Journal of Geodesy*, *85*(7), 395–413. https://doi.org/10.1007/s00190-010-0434-y

Teke, K., Kayıkçı, E. T., Böhm, J., & Schuh, H. (2012). Modelling very long baseline interferometry (VLBI) observations. *Journal of Geodesy and Geoinformation*, *1*(1), 17–26. https://doi.org/10.9733/jgg.120512.1

Teke, K., Nilsson, T., Böhm, J., Hobiger, T., Steigenberger, P., García-Espada, S., et al. (2013). Troposphere delays from space geodetic techniques, water vapor radiometers, and numerical weather models over a series of continuous VLBI campaigns. *Journal of Geodesy*, *87*(10–12), 981–1001. https://doi.org/10.1007/s00190-013-0662-z

Thaller, D., Tesmer, V., Dach, R., Krügel, M., Rothacher, M., & Steigenberger, P. (2008). Combining VLBI Intensive with GPS Rapid solutions for deriving a stable UT time series. In *Paper presented at the 5th IVS general meeting proceedings, St. Petersburg*. https://ivscc.gsfc.nasa.gov/publications/gm2008/thaller.pdf

Wang, J. (2021). *Integrated processing of GNSS and VLBI on the observation level*. Doctoral Thesis. Technische Universität Berlin, Berlin, Germany. https://doi.org/10.14279/depositonce-12513

Wang, J., Ge, M., Glaser, S., Balidakis, K., Heinkelmann, R., & Schuh, H. (2022). Improving VLBI analysis by tropospheric ties in GNSS and VLBI integrated processing. *Journal of Geodesy*, *96*(4), 32. https://doi.org/10.1007/s00190-022-01615-y

Wang, J., & Liu, Z. (2019). Improving GNSS PPP accuracy through WVR PWV augmentation. *Journal of Geodesy*, *93*(9), 1685–1705. https://doi.org/10.1007/s00190-019-01278-2

Wang, J., Wu, Z., Semmling, M., Zus, F., Gerland, S., Ramatschi, M., et al. (2019). Retrieving precipitable water vapor from shipborne multi-GNSS observations. *Geophysical Research Letters*, *46*(9), 5000–5008. https://doi.org/10.1029/2019gl082136

Zajdel, R., Sośnica, K., Bury, G., Dach, R., & Prange, L. (2020). System-specific systematic errors in Earth rotation parameters derived from GPS, GLONASS, and Galileo. *GPS Solutions*, *24*(3), 74. https://doi.org/10.1007/s10291-020-00989-w

Zuo, X., Jiang, X., Li, P., Wang, J., Ge, M., & Schuh, H. (2021). A square root information filter for multi-GNSS real-time precise clock estimation. *Satellite Navigation*, *2*(1), 28. https://doi.org/10.1186/s43020-021-00060-0

21699356, 2022, 11, Downloaded from https://agupubs.onlinelibrary.wiley.com/doi/10.1029/2022JB025228 by Helmholtz-Zentrum Potsdam GFZ, Wiley Online Library on [28/11/2022]. See the Terms and Conditions (https://onlinelibrary.wiley.com/terms-and-conditions) on Wiley Online Library for rules of use; OA articles are governed by the applicable Creative Commons License